

**Expression and function of Rab3 interacting molecules
and clarin-1 in inner hair cells**

Dissertation
for the award of the degree
Doctor rerum naturalium
of the Georg August Universität Göttingen

within the doctoral program (Sensory and Motor Neuroscience)
of the Georg-August-University School of Science (GAUSS)

Submitted by
Tomoko Oshima-Takago
From Hokkaido, Japan

Göttingen, 2013

Thesis Committee:

Prof. Dr. Tobias Moser

InnerEarLab, Department of Otolaryngology, University Medical Center Göttingen

Prof. Dr. Martin Göpfert

Cellular Neurobiology, Schwann-Schleiden Research Center, University of Göttingen

Prof. Dr. Georg Klump

Animal Physiology & Behavior Group, Department for Neuroscience, School of
Medicine and Health Sciences, Carl von Ossietzky University Oldenburg

Examination Board:

Prof. Dr. Erwin Neher

Membrane biophysics group, Max Planck Institute for Biophysical Chemistry

Dr. Dr. Oliver Schlüter

Molecular Neurobiology Lab, European Neuroscience Institute Göttingen

Dr. Camin Dean

Trans-synaptic Signaling, European Neuroscience Institute Göttingen

Date of oral examination: 12 March, 2013

Declaration

I hereby declare that I wrote this thesis for the degree of Doctor rerum naturalium
'Expression and function of Rab3 interacting molecules and clarin-1 in inner hair cells'
independently and with no other sources and aids than quoted.

Göttingen, 2013

Tomoko Oshima-Takago

Table of Contents

1. Introduction	1
1.1 Hearing and the auditory system	1
1.1.1 The mammalian ear	1
1.1.2 The cochlea	2
1.1.3 The organ of Corti	3
1.1.4 The inner hair cell (IHC)	6
1.1.5 Molecular anatomy and physiology of the inner hair cell ribbon synapse	10
1.2 Expression and function of Rab3 interacting molecules (RIMs) at presynaptic active zones of the IHCs	12
1.3 Clarin-1 and Usher syndrome type IIIA	15
1.3.1 Usher syndrome and Usher proteins	15
1.3.2 Expression and function of clarin-1 at the IHC ribbon synapse	18
2. Materials and Methods	20
2.1 Animals	20
2.2 Single-cell nested RT-PCR	20
2.3 Immunohistochemistry	21
2.4 Patch-clamp recording	22
2.5 Auditory brainstem responses (ABRs) and distortion-product otoacoustic Emission (DPOAEs)	23
2.6 Statistics	24
3. Results	25
3.1 Probing expression and function of RIM proteins in the IHCs	25
3.1.1 Mature IHCs express RIM2 α and RIM3 γ at their active zones after the onset of hearing	25
3.1.2 Disruption of RIM2 α reduces presynaptic Ca ²⁺ currents and exocytic membrane capacitance change	28
3.1.3 Auditory systems consequences of the disruption of RIM2 α	31
3.2 Probing presynaptic function of clarin-1 at the IHC ribbon synapse	32

4. Discussion	34
4.1 RIM2 α regulates L-type Ca ²⁺ current and Ca ²⁺ -triggered exocytosis at the IHC ribbon synapse	34
4.2 Discrepancy between the <i>in vitro</i> finding of impaired vesicle replenishment with reduced Ca ²⁺ currents and the <i>in vivo</i> finding of relatively intact auditory brainstem responses	36
4.3 Clarin-1 is dispensable for the ribbon synapse development and function	38
5. References	40
Abbreviations	55
6. Acknowledgements	57
7. Curriculum Vitae	59

Introduction

1. Introduction

1.1 Hearing and the auditory system

Hearing is one of the five senses and is essential for communications with others. It enables humans to transfer information and exchange ideas and thoughts. In other vertebrates, sound localization is also indispensable for survival and reproduction.

Sound is an oscillation of pressure waves propagated via a gas, liquid or solid medium. Its frequency and intensity are fundamental features for analyzing voices and for comprehending speech. Animals equipped with a pair of hearing organs utilize two additional features of sound, i.e. interaural time difference and interaural level difference, for localizing a sound source and analysis of an acoustic scene. Hearing is enabled by the auditory system, which includes the outer, middle, and inner ear, the auditory nerve as well as the central auditory pathway up to the auditory cortex.

1.1.1 The mammalian ear

The external ear, which is composed of the auricle and external auditory meatus, gathers acoustic stimuli and focuses them on the tympanic membrane. In humans, the external ear has a resonant frequency of around 3 kHz (Shaw, 1974). The external auditory meatus ends at the tympanic membrane, which compartmentalizes the outer and middle ear (see Figure 1 for a schematic representation).

The middle ear is an air-filled cavity, containing three tiny ossicles called malleus, incus, and stapes. These ossicles transmit the sound vibration from the comparatively large, low impedance tympanic membrane to the much smaller, high impedance oval window. This converts the low pressure, large displacement of the airborne acoustic stimuli into a high pressure, small displacement of the fluid in the cochlea. Thus, the middle ear plays an important role known as impedance matching (Wever and Lawrence, 1954).

The inner ear is a complex structure, which consists of two parts: the organ of hearing, the cochlea, and the vestibular apparatus. The vestibular apparatus further consists of the saccule and the utricle, which detect linear acceleration and head position,

Introduction

as well as of the semicircular canals, which detect angular acceleration (I hereafter mention nothing about the vestibular apparatus in this thesis).

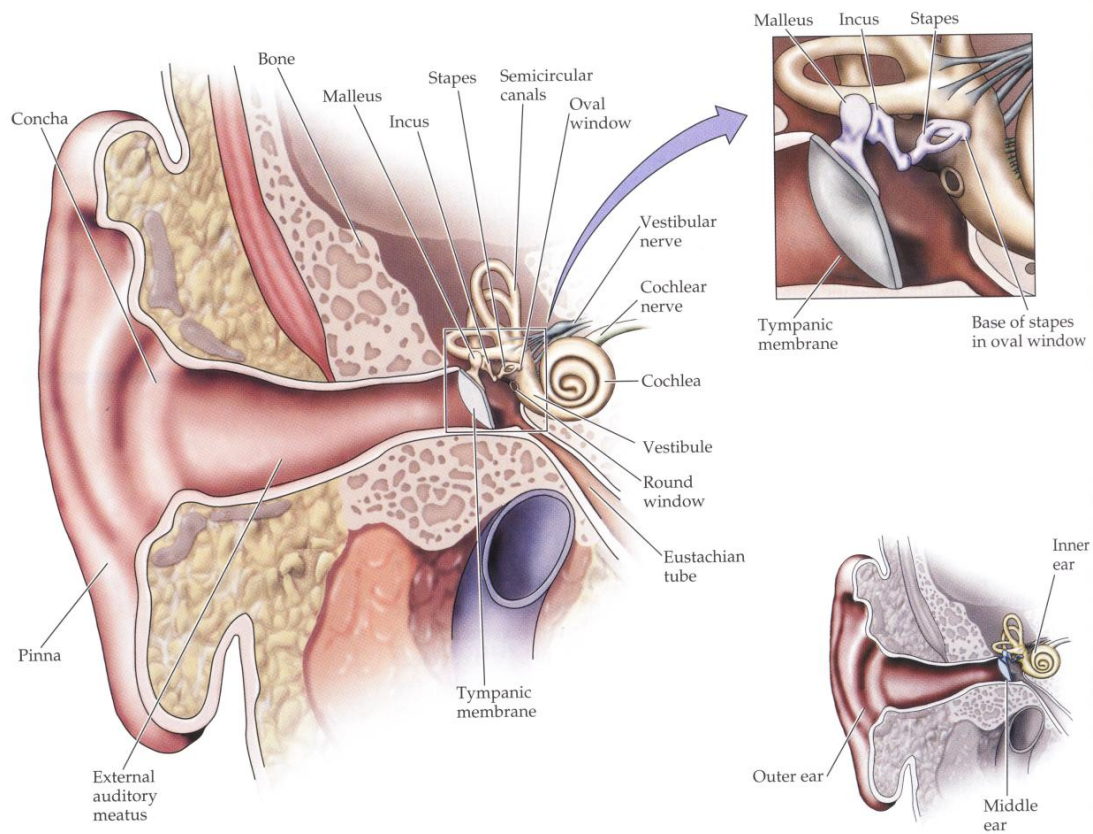


Figure 1 The human ear

The cross section of the human ear exposes the outer, middle, and inner ear as well as the eighth cranial nerve comprising the cochlear nerve and the vestibular nerve (left). After the sound waves vibrate the tympanic membrane, this energy is transferred via the three ear ossicles (malleus, incus, and stapes) to the oval window of the cochlea (upper right).

Adopted from Purves et al., 2004.

1.1.2 The cochlea

The cochlea derives its name from the *Cochlea*, the Latin word for snail, because of its unique coiled structure. The number of turns varies among species: in human it is 2.5, in mouse 1.75, and in guinea pig 4. The size of the human cochlea is 10 mm in width and

Introduction

5 mm from the base to the apex, and the coiled basilar membrane is approximately 35 mm in length, when uncoiled.

Inside the bony wall of cochlea, there are three partitioned compartments: scala vestibuli, scala media, and scala tympani. The scala vestibuli stands superior to the scala media with Reissner's membrane dividing them and the scala tympani stands inferior to the scala media with the basilar membrane dividing them. The scala vestibuli and the scala tympani communicate with each other via an opening known as helicotrema located at the very top of the cochlea apex, contain a common fluid called perilymph, which is similar to the extracellular fluid in composition, and are equipotential to the extracellular fluid elsewhere in the body. The scala media forms the middle compartment of the cochlea. However, it does not communicate with the other two compartments and contains a special fluid called endolymph, which is similar to the intracellular fluid with a high concentration of K^+ (157 mM, Wangemann and Schacht, 1996). This is produced by active transport of K^+ through the stria vascularis, generating a high positive potential (+ 80 mV, von Békésy, 1952) called endocochlear potential in the endolymph, which serves as a strong driving force for K^+ movement across the stereocilia on the hair cells (Hibino et al., 2010).

When the vibration of the stapes is transmitted to the scala vestibuli via the membranous opening called oval window, the fluid in the cochlea is displaced towards the other side, which contains another membranous opening, the round window, and is thus transmitted onto the scala tympani. This flow causes vertical movements of the basilar membrane, creating a travelling wave of the basilar membrane towards the cochlear apex. Here, the basilar membrane is tuned in its properties; it is thick, narrow and stiff in the base, but gets thinner, broader and more elastic towards the apex. Due to this gradation of the properties, high frequency sound leads the maximal basilar membrane vibration in the base and low frequency sound leads the maximal vibration in the apex. This micromechanical process is the first stage for the sound analysis in the auditory system, and even without active cellular contribution results in a rough mapping of sound onto tonotopic locations of the basilar membrane (for review, see Purves et al., 2004).

Introduction

1.1.3 The organ of Corti

The organ of Corti is a highly specialized structure situated on the basilar membrane with the function to convert acoustic signals into electrical signals. It contains a single row of inner hair cells (IHCs), three rows of outer hair cells (OHCs) and several kinds of supporting cells such as Deiter's cells, Hensen's cells, phalangeal cells, and pillar cells (Figure 1).

The OHCs have a cylindrical shape and play a role in amplification of sound energy via an active process (for review, see Hudspeth et al., 1997; Dallos and Fakler, 2002). On the apical surface, they have V- or W-formed hair bundles (stereocilia) attaching to the tectrial membrane. Vertical movement of the basilar membrane turns into deflection of stereocilia, causing opening/closing of mechanotransduction (MET) channels to depolarize/hyperpolarize the OHCs via cation influx (mainly K^+). This change in membrane potential drives an electromotility in the OHCs: depolarization causes cell contraction, in contrast, hyperpolarization causes cell elongation via a conformational change in the motor protein prestin (Zheng et al., 2000). The electromotility in the OHCs, indeed, underlies the cochlear amplification (Liberman et al., 2002).

Supporting cells play roles in homeostasis and mechanical support of the organ of Corti. In addition to these functions, recent studies revealed that they have a potential to trans-differentiate into new hair cells under specific conditions (White et al., 2006).

The organ of Corti receives afferent innervation by type I and type II spiral ganglion neurons (SGNs), which form auditory nerve fibers. In mature mice each IHC contacts with 5- 20 afferent dendrites of type I SGNs, a single type I SGN seems to receive input from a single IHC through a single active zone of the ribbon-type afferent synapse (e.g. Meyer et al., 2009). *L*-glutamate, a neurotransmitter at this synapse, is released from IHCs through the process of synaptic vesicle exocytosis and activates AMPA-type glutamate receptors on the type I SGNs to generate action potentials. This signal is relayed through the auditory pathway up to the auditory cortex. Type II SGNs receive inputs from 15- 20 OHCs (Spoendlin et al., 1972), which also release *L*-glutamate (Weisz et al., 2010).

The organ of Corti also receives efferent innervation from the olivocochlear system.

Introduction

The olivocochlear system has two pathways: the medial olivocochlear (MOC) pathway arising from the contralateral ventral nucleus of the trapezoid body and the lateral olivocochlear (LOC) pathway arising from the ipsilateral lateral superior olive (Guinan et al., 1984). The projection pattern of the MOC fibers and the LOC fibers varies with development. At the early stage of development, the MOC fibers project to the IHCs alone, while the projection of LOC fibers is unknown. At the intermediate stage, the MOC fibers project to both IHCs and OHCs, while the LOC fibers project to IHC region alone. Finally at the late stage of development, the MOC fibers project to OHCs, while the LOC fibers project to the afferent dendrites of IHCs (for review, see Simmons, 2002). The olivocochlear system employs predominantly acetylcholine (ACh) as its neurotransmitter to hyperpolarize the targeting cells via activation of $\alpha 9$ (Elgoyhen et al., 1994; Vetter et al., 1999) and $\alpha 10$ (Vetter et al., 2007) nicotinic ACh receptors concomitant with subsequent activation of small conductance Ca^{2+} -activated K^{+} channels (Yugas and Fuchs, 1999; Oliver et al., 2000). However, the LOC system additionally seems to employ dopamine as its neurotransmitter to activate dopamine receptors on the afferent dendrites of type I SGNs (Eybalin et al., 1993; Darrow et al., 2006). Efferents are believed to modulate the spontaneous activity of IHCs before the hearing onset (Glowatzki and Fuchs, 2000) and type I SGN activity after the hearing onset (Ruel et al., 2001) as well as the motility of OHCs for negative control of the cochlear amplifier via a motor protein prestin (Zheng et al., 2000).

Introduction

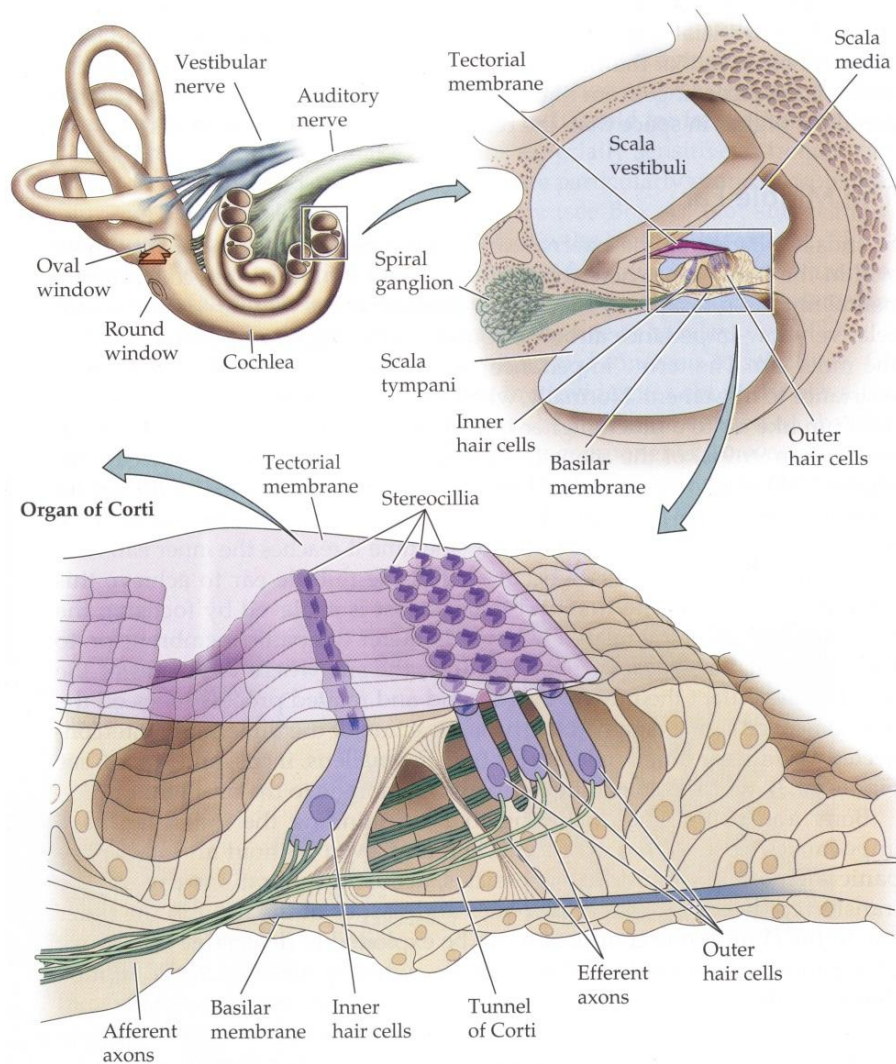


Figure 2 The cochlea and the organ of Corti

The cross section of the membranous labyrinth (top left) exposes three partitions of cochlea: scala vestibuli, scala media, and scala tympani (top right). The organ of Corti, a specialized structure for auditory transduction, is located between the tectorial membrane and the basilar membrane (bottom). A single row of inner hair cells, three rows of outer hair cells, and surrounding supporting cells are seen.

Adopted from Purves et al., 2004.

1.1.4 The inner hair cell (IHC)

The IHC is the genuine sensory cell of the organ of Corti, transducing auditory stimuli into a neural signal at its synapses with SGNs. It has a pear-like shape and 2-3 rows of

Introduction

stereocilia on the apical surface (hair bundle). The stereocilia amount to 20-50 in each IHC, depending on species and location (for review, see Raphael and Altschuler, 2003), and contain actin-filament cores (Sobin and Flock, 1983). The top of each stereocilium is connected to the lateral surface of its neighboring hair bundle through a tip-link filament, which is primarily composed of Cadherin 23 (Siemens et al., 2004; Sollner et al., 2004) and Protocadherin 15 (for review, see Müller, 2008). Since the tip links and mechano-electrical transduction (MET) channels are directly connected to each other, deflections of the hair bundle leading to changes in tension of the tip link filaments directly gate the MET channels. A displacement towards the kinocilium (or longest stereocilia) increases tension of tip links, opens MET channels, and allows cation influx (mainly K^+) to cause a depolarization in the IHC, which is termed a receptor potential. On the contrary, a deflection towards the opposite side (shortest stereocilia) decreases tension of tip links, closes MET channels, and shuts off cation influx to set the membrane potential to more negative values (for review, see Hudspeth, 1997). This receptor potential triggers the opening of voltage-gated Ca^{2+} channels at the ribbon-type synapses, further leading to exocytosis of synaptic vesicles at the active zones.

In addition to the MET channels, the IHCs express voltage-gated Ca^{2+} channels and K^+ channels (for review, see Kros, 1996).

While presynaptic Ca^{2+} currents at the conventional CNS synapses are carried by P/Q-, N-, and R-type Ca^{2+} channels, that at the IHC afferent synapse is carried by L-type Ca^{2+} channels (predominantly $Ca_v1.3$ ($\alpha 1D$) Ca^{2+} channels, Platzner et al., 2000; Brandt et al., 2003). The L-type Ca^{2+} channels have an advantageous feature: they remain active upon prolonged depolarization by their relatively little inactivation (Moser and Beutner, 2000; Ricci and Schnee, 2003; Yang et al., 2006; Cui et al., 2007; Grant et al., 2008). The L-type Ca^{2+} channels are clustered at the release sites of the IHC ribbon synapse (Roberts et al., 1990; Zenisek et al., 2003; Brandt et al., 2005), allowing nanodomain control of synaptic vesicle exocytosis (Brandt et al., 2005). Interestingly, the number of L-type Ca^{2+} channels varies among ribbon synapses within a single IHC, which could contribute to the heterogeneous response properties of the auditory nerve fibers to the sound. The Ca^{2+} current density undergoes a developmental

Introduction

change; it reaches the maximum level at P6 and decreases afterwards (Beutner and Moser, 2001). Just recently, two families were identified that have sinoatrial node dysfunction and deafness (termed SANDD syndrome) due to a mutation in CACNA1D encoding $Ca_v1.3$ ($\alpha1D$) Ca^{2+} channels (Baig et al., 2011).

Presynaptic K^+ currents are carried by large-conductance Ca^{2+} -activated potassium (BK) channels, K_v -type voltage-gated potassium channels, voltage-gated potassium channel of the KQT-like subfamily, member 4 (KCNQ4), and small-conductance Ca^{2+} -activated potassium (SK) channels. The BK current, which is also known as $I_{K,f}$, due to a fast activation, shapes the sound-evoked receptor potential in the mammalian IHCs (Oliver et al., 2006) and contributes to frequency-tuning in the non-mammalian vertebrates IHCs (Ramanathan et al., 1999). Interestingly, it is not until the onset of hearing that they begin to be expressed (Kros et al., 1998). The K_v -type potassium current, which is known as $I_{K,s}$ due to a slower activation, mediates a delayed rectifier conductance (Kros et al., 1998; Marcotti et al., 2003). The KCNQ4 ($K_v7.4$) potassium channel, which is affected in autosomal dominant hereditary deafness type 2 (DFNA2), carries a low-voltage activated, slow delayed rectifier K^+ conductance, $I_{K,n}$, and contributes to the resting membrane potential (Marcotti et al., 2003; Oliver et al., 2003; Kharkovets et al., 2006). SK channels are expressed on IHCs transiently until the onset of hearing (Katz et al., 2004; Marcotti et al., 2004b), and are essential for cholinergic function of efferent inhibition (Fuchs and Murrow, 1992; Kong et al., 2008).

Introduction

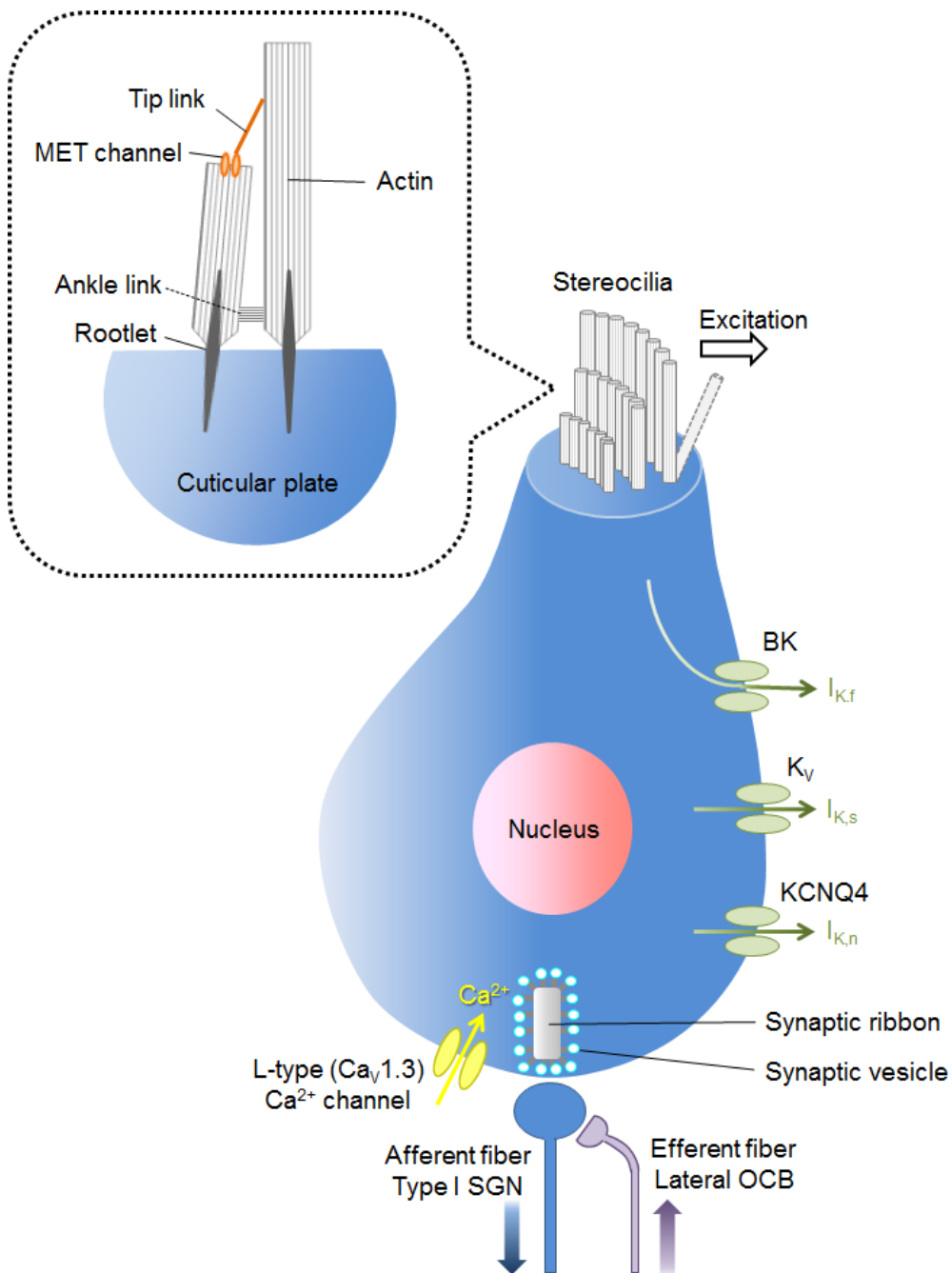


Figure 3 The inner hair cell with its ion channels as well as afferent and efferent innervating fibers

The IHC expresses the mechano-electrical transduction (MET) channel (depicted in orange), three classes of K^+ channels (BK, K_V , and KCNQ4, green), L-type ($Ca_v1.3$) Ca^{2+} channels (yellow). Note that the IHC is innervated by afferent fibers of type I spiral ganglion neurons (blue), which further innervated by lateral olivocochlear efferents (purple). Modified from Bulankina and Moser, 2012.

Introduction

1.1.5 Molecular anatomy and physiology of the inner hair cell ribbon synapse

The most characteristic property of the IHC afferent synapse is the synaptic ribbon, a submicron-sized electron-dense structure where 125 (in electron-microscopic study) or 200 (in 4pi study) synaptic vesicles are tethered (for review, see Nouvian et al., 2006). The synaptic ribbon is found among the retinal photoreceptors and bipolar cells, auditory and vestibular hair cells, and pinealocytes (for review, see Lenzi and von Gersdorff, 2001; Fuchs et al., 2003; Lagnado et al., 2003; Sterling and Matthews, 2005; Matthews and Fuchs, 2010). It is also found in the hair cells and electroreceptors of the lateral line in fish and amphibians (Katz et al., 1993). Thus, the synaptic ribbon seems to be present wherever the system requires exocytosis evoked by graded depolarization to cover a wide dynamic range of stimuli and where a high, sustained rate of release is needed.

The synaptic ribbons in the mammalian cochlea are relatively small (less than 200 nm in width), Moser et al., 2006). In the mammalian cochlea, more than 100 synaptic vesicles are tethered to the ribbon (Nouvian et al., 2006) and several tens of L-type Ca^{2+} channels are present at these active zones (Brandt et al., 2005; Meyer et al., 2009; Zampini et al., 2010), where synaptic transmission occurs. The number of docked synaptic vesicles is estimated to be approximately 10-20 (Pangršič et al., 2010) and this seems enough to support a rapid burst of release at the onset of stimulus.

The molecular components of the synaptic ribbon have recently begun to be deciphered. The protein RIBEYE is a major constituent of the ribbon and has two domains. Its B domain is almost identical to a ubiquitous transcription factor, C-terminal binding protein 2 (CtBP2) and bears enzymatic activity (Schwarz et al., 2011), while its A domain mediates homophilic interactions (Magupali et al., 2008). In addition, scaffolding proteins such as bassoon and piccolo are present in synaptic ribbons. Recent studies have shown that bassoon anchors the ribbons to the active zones (Dick et al., 2001, 2003; Khimich et al., 2005; Frank et al., 2010). Moreover, Rab3 interacting molecules (RIMs, Wang et al., 1997) are present at the active zones of retinal photoreceptors (tom Dieck 2005) and immature IHCs (Gebhart et al., 2010),

Introduction

while it was stated to be absent from the active zones of mature IHCs (Gebhart et al., 2010).

Although the precise functions of the synaptic ribbon remain to be addressed, there have been a few hypotheses for them. One is that the ribbon functions as a ‘conveyor belt’ to move the vesicles in the upper rows down to the active zone for continuous vesicle supply (Bunt, 1971). Another is that the ribbon functions to enable a large RRP of synaptic vesicles at the active zone (Khimich et al., 2005; Moser et al., 2006b).

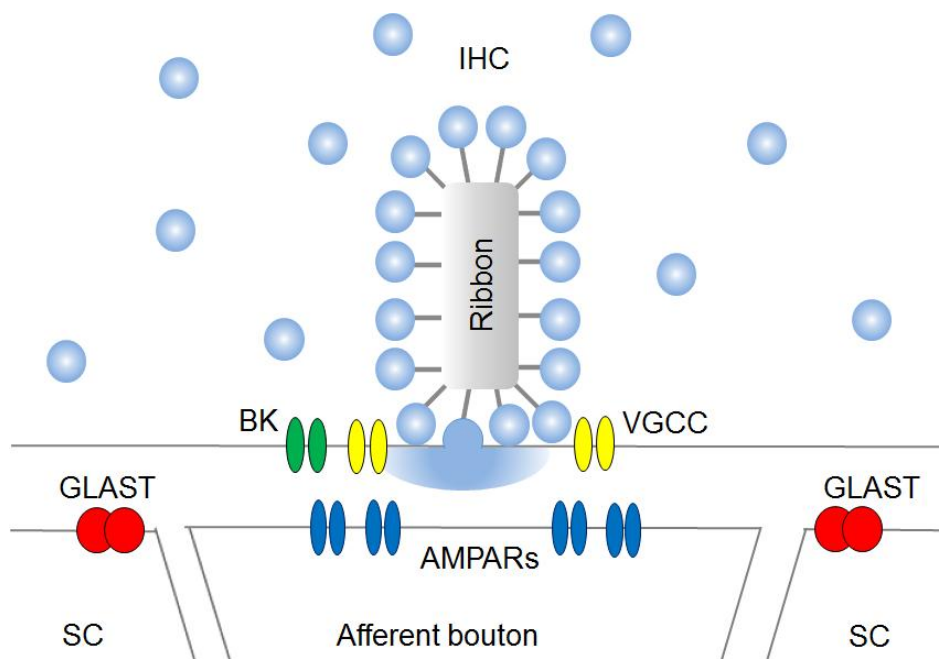


Figure 4 The inner hair cell ribbon synapse

The synaptic ribbon, an electron-dense structure located beneath the presynaptic plasma membrane, tethers a number of synaptic vesicles (pale blue). L-type ($Ca_v1.3$) Ca^{2+} channels (VGCCs, yellow) and large-BK-type K^+ channels (green) are clustered near the synaptic ribbons. AMPA-type glutamate receptors (blue) are expressed on the surface of postsynaptic afferent boutons for binding to neurotransmitter glutamate, while glutamate transporters (GLAST, red) are expressed on the surface of supporting cells (SCs) for clearance of glutamate in the synaptic cleft. Modified from Fuchs et al., 2003.

Introduction

1.2 Expression and function of RIMs at presynaptic active zones of the IHCs

The active zone is a specialized structure in the presynaptic plasma membrane where synaptic vesicles undergo docking, priming, and fusion in order to release their neurotransmitters onto the postsynaptic neurons. A variety of proteins are involved in this process (for review, see Südhof and Rizo, 2011; Schoch and Gundelfinger, 2006). Among these are the Rab3-interacting molecules (RIMs), which are major active zone proteins and are ubiquitously expressed at central synapses.

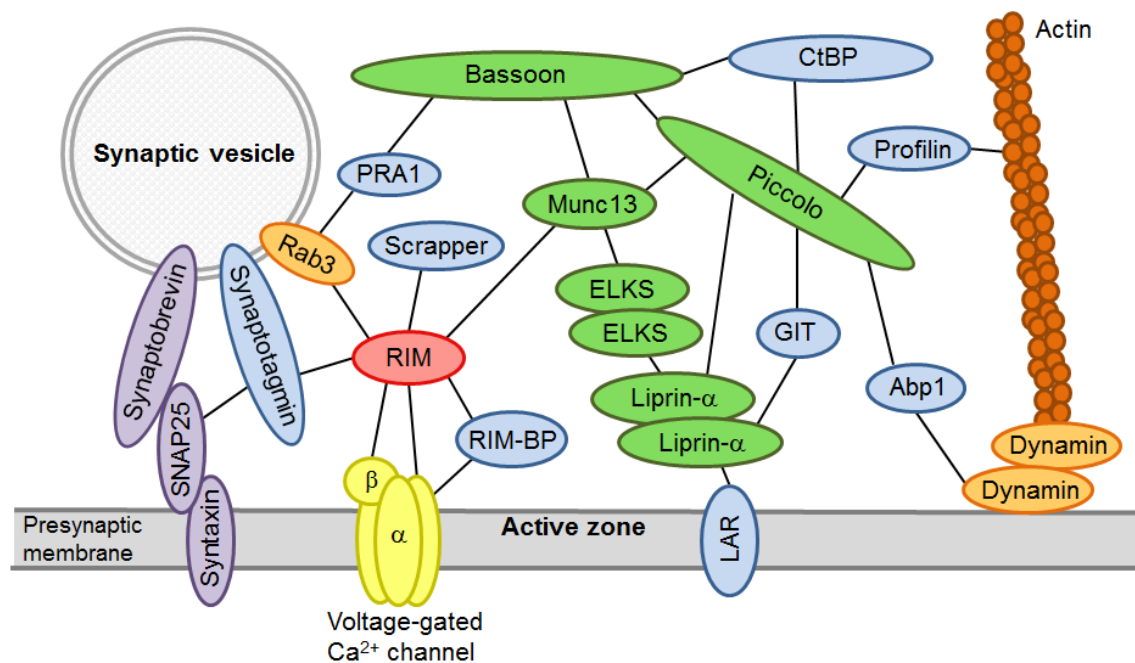


Figure 5 The active zone proteins

Modified from Mittelstadt et al., 2010

The RIMs are composed of the multi-domain α -RIMs and β -RIMs (RIM1 α , RIM1 β , RIM2 α and RIM2 β) as well as the shorter γ -RIMs (RIM2 γ , RIM3 γ and RIM4 γ). α -RIMs contain a full set of domains: a helix α 1 and a zinc finger domain in the N-terminus, a PDZ-domain in the center, two C₂-domains (C₂A and C₂B) and a proline-rich sequence in the C-terminus (Wang et al., 2000). RIM1 β is similar to RIM1 α except that RIM1 β lacks the helix α 1, while RIM2 β is similar to RIM2 α except that RIM2 β lacks the helix α 1 and the zinc finger domain. γ -RIMs only contain an isoform-specific N-terminus and the C₂B domain (Wang et al., 1997).

Introduction

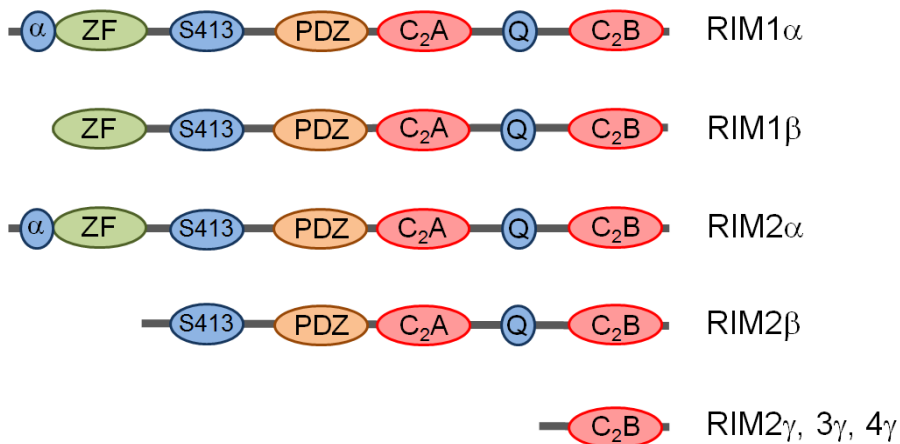


Figure 6 Domain components of RIM isoforms

(a) helix α 1; (ZF) zinc finger domain; (S413) serine 413, phosphorylation site for PKA; (PDZ) PSD95, Dlg, and ZO-1/2-like domain; (C₂) PKC conserved region 2; (Q) proline-rich sequence. Modified from Mittelstadt et al., 2010.

Remarkably RIMs interact with remaining active zone proteins such as Munc13, Bassoon, Piccolo, ELKS and Liprin- α (for review, see Mittelstaedt et al., 2010). Moreover, PDZ domains of RIMs directly bind to the α -subunits of P/Q- and N-type Ca²⁺ channels (Kaeser et al., 2010). In addition, RIMs are linked to P/Q-, N-, and L-type Ca²⁺ channels via an interaction with RIM-binding proteins (RIM-BPs) through their proline-rich domains (Hibino et al., 2002).

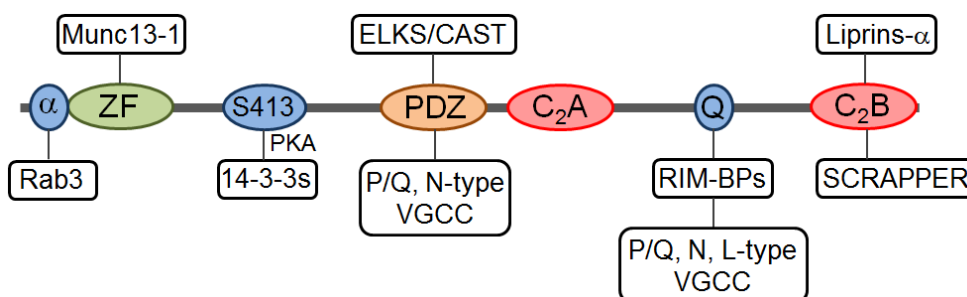


Figure 7 RIMs interact with multiple other active zone proteins in central synapses

(a) helix α 1; (ZF) zinc finger domain; (S413) serine 413, phosphorylation site for PKA; (PDZ) PSD95, Dlg, and ZO-1/2-like domain; (C₂) PKC conserved region 2; (Q) proline-rich sequence. Modified from Mittelstadt et al., 2010.

Introduction

The RIMs play essential roles in neurotransmitter release and synaptic plasticity. Several recent studies have shown that RIM1 and 2 regulate the docking/priming step of the release process and tether P/Q- and N-type Ca^{2+} channels to the active zones in hippocampal cultured neurons (Kaeser et al., 2010) as well as at the calyx of Held synapse (Han et al., 2011). RIM1 α alone not only controls release probability but also changes both short- and long-term synaptic plasticity in the hippocampus (Schoch et al., 2002; Castillo et al., 2002, Calakos et al., 2004). However, deletion of RIM2 α failed to show any synaptic phenotypes in the hippocampus. Knockout of both RIM1 α and RIM2 α causes perinatal lethality without changing synaptic structure and formation, although deletion of either RIM1 α or RIM2 α does not cause this perinatal lethality (Schoch et al., 2006).

Compared to CNS synapses, the expression and function of RIMs in the sensory epithelium have not been characterized. Expression of RIMs was detected in the mouse retina, although their function was not elucidated (tom Dieck et al., 2005; Deguchi-Tawarada et al., 2006). Notably the distribution profiles of the RIM proteins are different between the wild-type retina and the ribbon-deficient Bassoon mutant retina: both RIM1 and RIM2 colocalize with RIBEYE at the wild-type photoreceptor terminal, while only RIM1, not RIM2, colocalizes with RIBEYE at the mutant photoreceptor, suggesting that RIM1 localizes to the synaptic ribbon, but RIM2 is present at the plasma membrane of the active zone (tom Dieck et al., 2005). A recent study indicated that RIM2 α , but not other isoforms of RIMs, is expressed in IHCs, however, only before hearing onset (Gebhart et al., 2010). In order to provide more information on the role of RIMs in hearing, I probed the role of RIMs at the first auditory synapse employing RIM knockout animals.

Introduction

1.3 Clarin-1 and Usher syndrome type IIIA

1.3.1 Usher syndrome and Usher proteins

Usher syndrome (USH) is an autosomal recessive disorder, which was named after the English medical doctor Charles Usher (Usher, 1914), although it had been first reported by the German medical doctor Albrecht von Graefe as retinitis pigmentosa in combination with deafness (von Graefe, 1858). Among the around 40 kinds of hereditary disorders which present deafness and blindness, USH is the most frequent with approximately 50 % of all cases (Saihan et al., 2009). USH is clinically classified into three types according to the extent and the onset of deafness as well as the presence of vestibular dysfunction (Smith et al., 1994). To date, at least 10 genetic loci have been mapped for USH and in most cases, the responsible genes have been identified (Weil et al., 1995; Verpy et al., 2000; Bitner-Glindzicz et al., 2000; Wayne et al., 1996; Bork et al., 2001; Bolz et al., 2001; Chaib et al., 1997; Ahmed et al., 2001, 2009; Alagramam et al., 2001; Mustapha et al., 2002; Weil et al., 2003; Kimberling et al., 1990; Eudy et al., 1998; Pieke-Dahl et al., 2000; Weston et al., 2004; Ebermann et al., 2007, 2010; Sankita et al., 1995).

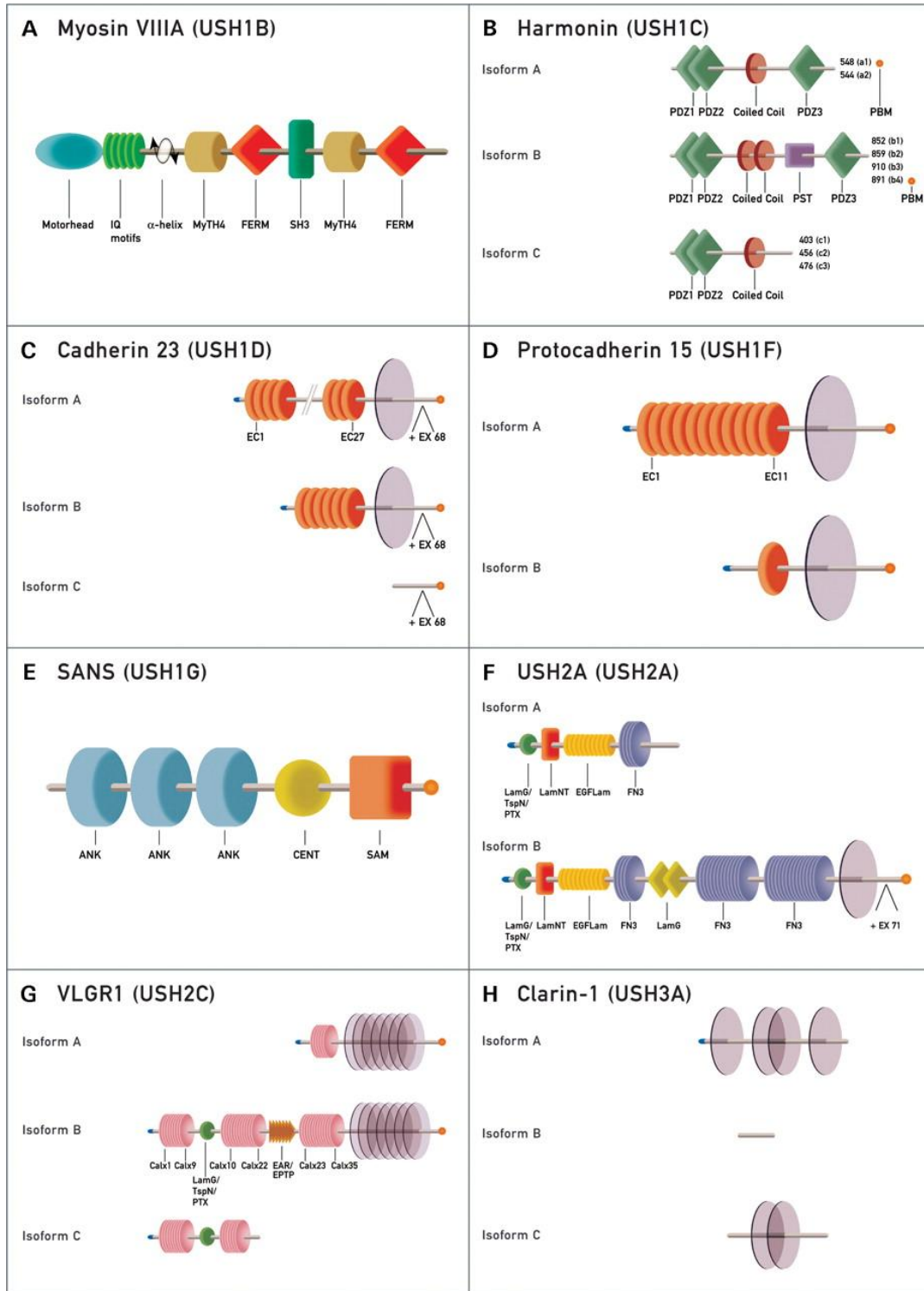
USH type I patients are born profoundly deaf and have severe vestibular dysfunction. They present with progressive vision impairment afterwards by the age of ten. To date, seven genetic loci (USH1B-H) have been mapped for this subtype, and five causative genes for USH type I have been identified, namely myosin VIIa (*MYO7A*, USH1B), harmonin (*USH1C*, USH1C), cadherin 23 (*CDH23*, USH1D), protocadherin 15 (*PCDH15*, USH1F), and sans (*SANS*, USH1G).

USH type II patients are born moderately to severely deaf without vestibular dysfunction. Vision problems in USH type II progress more slowly compared to USH type I. The causative genes for USH type II are usherin (*USH2A*, USH2A), VLGR1 (*VLGR1*, USH2C) and whirlin (*WHRN*, USH2D).

USH type III patients are not born deaf, but may develop progressive hearing loss afterwards. The severity of auditory, vestibular or vision symptoms varies from person to person. The only identified causative gene for USH type III is clarin-1 (*CLRN1*), whose genetic locus is 3q21-q25 (Sankila et al., 1995). In USH type III patients, at least

Introduction

10 mutations in the CLRN1 gene have been detected (Joensuu et al., 2001; Adato et al., 2002; Fields et al., 2002; Ness et al., 2003; Aller et al., 2004; Sadeghi et al., 2005; Ebermann et al., 2007; Herrera et al., 2008).



Introduction

Figure 8 Usher proteins and their different isoforms

(A) The USH1B protein, myosin VIIa, is comprised of a motor head domain, five calmodulin-binding IQ motifs, two FERM domains, two MyTH4 domains and a Src homology 3 (SH3) domain. (B) The USH1C protein, harmonin, is comprised of at least two PDZ (PSD95, discs large, ZO-1) domains (PDZ1 and 2) and a coiled-coil domain. The class A isoform contains an additional PDZ domain (PDZ3). The class B isoform also contains this PDZ3 domain, a second coiled-coil domain and a proline, serine, threonine-rich region (PST). Isoforms A1 and B4 contain a C-terminal class I PDZ binding motif (PBM). (C) The USH1D protein, cadherin 23, has three different isoforms. The isoform A is comprised of 27 Ca^{2+} -binding extracellular cadherin domains (EC1-27), a transmembrane domain (grey disks) and a short intracellular domain with a C-terminal class I PBM. The isoform B is similar to the isoform A, but only contains the last six EC domains. The isoform C is comprised of the intracellular domain and C-terminal PBM. (D) The USH1F protein, protocadherin 15, is comprised of either eleven (isoform A) or one (isoform B) EC domain, a transmembrane domain and a C-terminal class I PBM. (E) The USH1G protein, SANS, is comprised of three ankyrin domains (ANK), a central region (CENT), a sterile alpha motif (SAM) and a C-terminal class I PBM. (F) Isoform A of the Usher 2A protein (USH2A) is comprised of an N-terminal thrombospondin/pentaxin/laminin G-like domain, a laminin N-terminal (LamNT) domain, ten laminin-type EGF-like (EGF Lam) and four fibronectin type III (FN3) domains. In addition to this region, Isoform B contains two laminin G (LamG), 28 FN3, a transmembrane domain and an intracellular domain with a C-terminal class I PBM. (G) Isoform B of the USH2C protein, the very large G-coupled protein receptor VLGR1, contains a thrombospondin/pentaxin/laminin G-like domain, 35 Ca^{2+} -binding calcium exchanger β (Calx) domains, seven EAR/EPTP repeats, a seven-transmembrane region and an intracellular domain containing a C-terminal class I PBM. (H) Clarin-1, the USH3A protein, contains four (isoform A), none (isoform B), or one transmembrane (isoform C) domain. Adopted from Kremer et al., 2006.

Introduction

Usher proteins undergo a wide range of mutual interactions (Figure 9). Among them, the USH1C protein harmonin plays a central role, interacting with most of the remaining USH proteins. Moreover, a recent study reported that harmonin reduces synaptic Ca^{2+} influx through $\text{Ca}_v1.3$ -type Ca^{2+} channels in IHCs (Gregory et al., 2011).

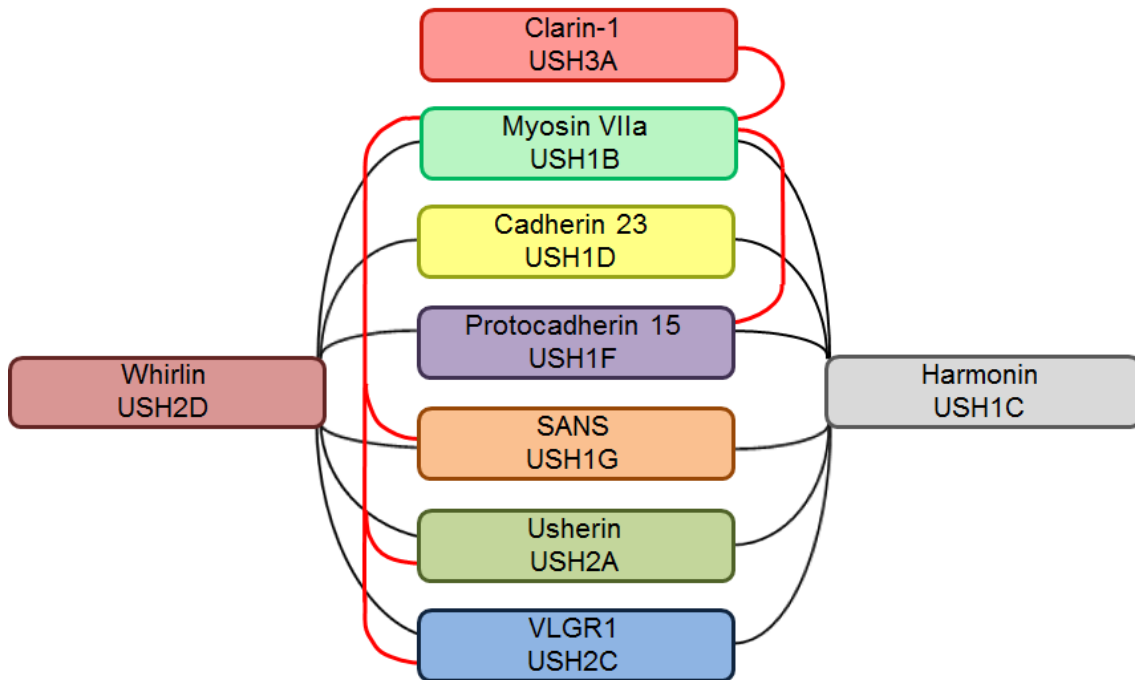


Figure 9 The Usher protein network

Currently known protein–protein interactions between different Usher proteins. Note that clarin-1 interacts with Myosin VIIa (Adato et al., 1999). Modified from Brown et al., 2008.

1.3.2 Expression and function of clarin-1 at the IHC ribbon synapse

Clarin-1, a member of four- transmembrane superfamily also containing tetraspanins and claudins, had been proposed to regulate hair cell synaptic transmission as well as the organization of actin filaments, on the basis of its expression at the synaptic and stereociliar sites (Adato et al., 2002; Tian et al., 2009; Geng et al., 2009; Zallocchi et al., 2009 and 2012). A preceding study found that the *CLRN1* knockout mouse, an animal model for USH type IIIA, develops profound hearing loss as well as vestibular dysfunction, and that the hair bundles are disrupted in *CLRN1*^{-/-} mice (Geng et al., 2009).

Introduction

Although the hair bundle disruption seemed to cause the mechano-electrical transduction deficit and mostly underlies the elevated ABR thresholds, a further involvement of synaptic deficits at the IHC afferent synapse was suggested on the basis of the observed delay in the peak latencies of ABRs in *CLRNI*^{-/-} mice (Geng et al., 2009). To test this hypothesis, I probed the presynaptic functions of clarin-1 knockout mice.

.

Materials and Methods

2. Material and Methods

2.1 Animals

The generation of knockout mice was previously described for *RIM2 α ^{-/-}* (Schoch et al., 2006) and for *Clrn1^{-/-}* (Geng et al., 2009), respectively. As controls, age-matched wild-type littermates were used. All experiments were complied with national animal care guidelines and approved by the University of Göttingen Board for Animal Welfare and the Animal Welfare Office of the State of Lower Saxony.

2.2 Single-cell nested RT-PCR

Wild-type C57BL6 mice at the age of postnatal days (P) 14 through 16 were used in this study. IHCs from the apical coils of freshly dissected organs of Corti were harvested after cleaning off supporting cells at a high bath perfusion rate (3 ml/min). Each individual IHC was aspirated and the pipette content was transferred into first strand cDNA synthesis mix containing after the dilution: 50 mM Tris-HCl, pH 8.3, 75 mM KCl, 5 mM MgCl₂, 5 mM DTT, 100 units of SuperScript II Reverse Transcriptase (Invitrogen, Carlsbad, CA) and 40 units RNaseOUT Ribonuclease inhibitor (Invitrogen). Reverse transcription was performed with oligo(dT)primers according to the manufacturer's instructions. Aspirated bath solution was used as a negative control. Each cDNA mix was used as a template for two subsequent PCR reactions with nested primers specific for RIM1 α - β , RIM2 α - γ , RIM3 γ , RIM4 γ , and otoferlin or RIBEYE (specific) cDNA. Primer sequences are listed in Table 1 and 2.

Materials and Methods

	fwd/rev	1st	nested
RIM1	forward	GAGGAACGAACGAGACAGATGAAA	GTCCGCCAAGTCATCAGATAGTGA
	reverse	TTTTTAACTTCTTGTGGCCGGACT	TTCTGCTTCTTCGAGACACAATGG
RIM2	forward	GCCTCTCAACTCAGCCAAAC	GATGGCAGCATGAACAGCTA
	reverse	CAGAGACGATTGGGAAGCTC	TAGGGAGGAAGGAGGGAAGA
RIM3	forward	TGGGAGCACCAACAGTAACA	AAGCCAGTTCAGTGACTTTCTGGA
	reverse	CATGTTTTCTTGGCCACCTT	GTTCTCCAGCAGGTAAGCCTTGAT
RIM4	forward	AACTGCCAGCTGCCTATATCAAG	TGTCTGCATTGCCAAGAAGAAAAC
	reverse	CGTAGTTTCCCCACACGATTACCT	GGGACTCTCAGGAAACAGAAGCAC

Table 1. Primers for RT-PCR/nested RT-PCR

	fwd/rev	1st	nested
RIM1 α	forward	CTCCCCCTATGCAAGAACTG	ACCGAGGAGGAGAGGAACAT
	reverse	GACCTTGATCGCTCTTGGAG	TTGTTGATCGCAGAGACAC
RIM1 β	forward	CAGAAGCTGTCCATTTTCC	CCTTCTGGAGCTTTCTGAGC
	reverse	GACCTTGATCGCTCTTGGAG	TTGTTGATCGCAGAGACAC
RIM2 α	forward	AGCAAGAGCAGAAGGGTGAT	CTGCAGCAACCTGATCAAAA
	reverse	TCCACATCTTCATCATCCACA	ATTGAGGCTCACGCTGAGAT
RIM2 β	forward	GCCAGGTCTGCAATTCTGTT	CGCTGAACAATGCAAGAAAA
	reverse	TCCACATCTTCATCATCCACA	ATTGAGGCTCACGCTGAGAT
RIM2 γ	forward	TCCATGCAGCGCTCTCAG	CAGCCTCTCTGCCTCTTTTG
	reverse	TAGCTGTTTCATGCTGCCATC/ TCCAGGAAATCACTGAACTGG	CCTCCTCTCTCCTTCATCT

Table 2. Subtype-specific primers for RT-PCR/nested RT-PCR

2.3 Immunohistochemistry

The freshly dissected apical cochlear turns from P9-17 wild-type C57Bl6 mice were fixed with 100 % methanol for 20 min at -20°C . Thereafter, the tissue was washed three

Materials and Methods

times for 10 min in PBS and blocked for 1 h in goat serum dilution buffer (GSDB) (16% normal goat serum, 450 mM NaCl, 0.3% Triton X-100, and 20 mM phosphate buffer, pH 7.4) in a wet chamber at room temperature. Primary antibodies were dissolved in GSDB and applied overnight at +4°C in a wet chamber. After washing three times for 10 min (wash buffer: 450 mM NaCl, 20 mM phosphate buffer, and 0.3% Triton X-100), the tissue was incubated with secondary antibodies in GSDB in a wet light-protected chamber for 1 h at room temperature. Then the preparations were washed three times for 10 min in wash buffer and one time for 10 min in 5 mM phosphate buffer, placed onto glass microscope slides with a drop of fluorescence mounting medium (Dako, Glostrup, Denmark), and covered with thin glass coverslips. The following antibodies were used: mouse IgG1 anti-CtBP2 (also recognizing the ribbon protein RIBEYE; 1:150; BD Biosciences), polyclonal rabbit antibody 1 against RIM 2, PDZ domain (1:200; Synaptic System, Göttingen, Germany), RIM3 γ (1:200, kindly provided by Prof. Dr. Susanne Schoch at University of Bonn) as well as secondary AlexaFluor488- and AlexaFluor568-labeled antibodies (1:200; Invitrogen). Confocal images were acquired using a laser scanning confocal microscope (TCS SP5, Leica, Wetzlar, Germany) with 488 nm (argon) and 561 nm (helium–neon) lasers for excitation and a 63 \times oil-immersion objective (1.4 numerical aperture; Leica). Whole-mount preparations of the organ of Corti provided the possibility to analyze several IHCs in a row (Khimich et al., 2005). Images were processed using NIH ImageJ software and assembled for display in Adobe Illustrator software (Adobe Systems).

2.4 Patch-clamp recording

For analyzing the IHC presynaptic function, I performed perforated patch-clamp recordings in apical coils of freshly dissected organs of Corti (Moser and Beutner, 2000) from *RIM2 α ^{-/-}* mice or *Clrn1^{-/-}* mice and their wild-type littermates (P13-19 for RIM2 α -related animals, P14-20 for Clrn-1-related animals). The pipette solution contained (in mM): 130 Cs-gluconate, 10 TEA-Cl, 10 4-AP (4-aminopyridine; Merck KGaA, Darmstadt, Germany), 1 MgCl₂, 10 HEPES (pH adjusted with HCl to 7.17, osmolarity ~ 290 mOsm/kg) and 300 μ g/ml amphotericin B (Calbiochem, La Jolla, CA)

Materials and Methods

dissolved in dimethyl sulfoxide (Invitrogen). The extracellular solution contained (in mM): 104 NaCl, 35 TEA-Cl, 2.8 KCl, 10 CaCl₂, 1 MgCl₂, 10 HEPES, 1 Cs gluconate, 5 4-AP, 11.1 D-glucose (pH adjusted with NaOH to 7.2, osmolarity ~ 300 mOsm).

Pipettes were prepared by a puller (P-97, Sutter Instruments Company, Novato, CA) with a resistance of 3-5 MΩ coated with Sylgard (Dow Corning, Midland, MI). An EPC-10 amplifier controlled by Pulse software (HEKA Elektronik, Lambrecht, Germany) was used for recordings from IHCs visualized by BX-50WI (Olympus, Tokyo, Japan) with a 40X magnification by an objective lens (Olympus).

All voltages were corrected for liquid-junction potentials. Currents were sampled at 20 kHz and low-pass filtered at 2 kHz. Cells that displayed a leak current exceeding –30 pA were discarded from analysis. Ca²⁺ currents were further isolated using a P/n protocol. Series resistance (R_S) was below 30 MΩ. Patch-clamp data were analyzed with Igor software (Wavemetrics, Portland, OR).

2.5 Auditory brainstem responses (ABRs) and distortion-product otoacoustic emission (DPOAE)

RIM2α^{-/-} and *RIM2α*^{+/+} mice (5-weeks-old to 8-weeks-old) were anesthetized by intraperitoneal injection of a combination of ketamine (100–125 μg/g) and xylazine (2.5–5 μg/g). The heart rate of anesthetized animals was constantly monitored by electrocardiogram (ECG). The body temperature was maintained constant at 37 °C using a rectal temperature-controlled heat blanket (Hugo Sachs Elektronik–Harvard Apparatus GmbH, Hugstetten, Germany). For stimulus generation, presentation, and data acquisition, we used the TDT II or III Systems (Tucker Davis Technologies, Alachua, FL) run by BioSig32 software (TDT) or MATLAB (Mathworks, Natick, MA) routines. Sound pressure levels are provided in decibels sound pressure level (SPL) rms (tonal stimuli) or decibels SPL peak equivalent (clicks) and were calibrated using a ¼ inch Brüel & Kjaer microphone (D 4039; Brüel & Kjaer, Nærum, Denmark). Stimuli were presented ipsilaterally in the free field using a JBL 2402 speaker (JBL, Northridge, CA).

Materials and Methods

For recording ABRs, the difference potential between vertex and mastoid subdermal needles was amplified (50,000 times), filtered (low pass, 4 kHz; high pass, 100 Hz) and sampled at a rate of 50 kHz for 20 ms, 2×2000 times to obtain two mean ABRs for each sound intensity. Hearing threshold was determined with 10 dB precision as the lowest stimulus intensity that evoked a reproducible response waveform in both traces by visual inspection.

For recording DPOAEs, a 24-bit sound card and the ED1/EC1 speaker system (Tucker David Technologies) were used to generate two primary tones f_1 and f_2 (f_2/f_1 ratio: 1.2). Primary tones were coupled into the ear canal by a custom-made probe containing an MKE 2 microphone (Sennheiser, Barleben bei Magdeburg, Germany) and adjusted to an intensity of 60 dB sound pressure level at the position of the ear drum as mimicked in a mouse ear coupler. The microphone signal was amplified (DMP3; M-audio, Hallbergmoos, Germany) and analyzed by fast Fourier transformation.

2.6 Statistics

Means are presented with their standard errors and were statistically compared using Student's unpaired, two-tailed t test, unless otherwise noted.

Results

3. Results

3.1 Probing expression and function of RIM proteins in the IHCs

3.1.1 Mature IHCs express RIM2 α and RIM3 γ at their active zones after the onset of hearing

To detect Rab3-interacting molecules (RIMs) mRNAs in IHCs of hearing mice, I performed nested single cell RT-PCR in collaboration with Dr. Friederike Predöhl. Among the 10 IHCs examined, all cells expressed otoferlin (positive control), 7 cells expressed RIM2 and RIM3 mRNAs, but none contained RIM1 or RIM4. In contrast, nested RT-PCR analysis of the whole organ of Corti showed expression of all isoforms of RIMs (Figure 10A). To further clarify the isoform-specific expression of RIM2, we analyzed another 10 IHCs. Among them, 9 cells expressed CtBP2 (positive control), 5 cells expressed RIM2 α mRNAs, but none contained RIM2 β or RIM2 γ (Figure 10B). Taken together, these results suggest that the IHCs in hearing mice express the isoforms RIM2 α and RIM3 γ .

To substantiate this finding, I performed immunohistochemical analysis of the expression of RIM2 α and RIM3 γ on whole mounts of the organ of Corti from hearing mice using anti-RIM2 and anti-RIM3 γ antibodies together with antibody directed against the nuclear protein CtBP2, which also detects RIBEYE, a major structural component of the synaptic ribbon (Schmitz et al., 2000, Khimich et al., 2005). As shown in Figure 10C-E, RIM2 and RIM3 γ immunofluorescence was observed within and around the base of the IHCs. Specifically, we found RIM2 and RIM3 γ immunofluorescence at CtBP2 labeled ribbon-type active zones, indicating that IHCs of hearing mice express RIM2 α and RIM3 γ isoforms at their active zones. Additional RIM2 immunofluorescence outside the IHCs most likely represented RIM expression in efferent nerve terminals, which display small conventional active zones, as well as unspecific labeling.

Results

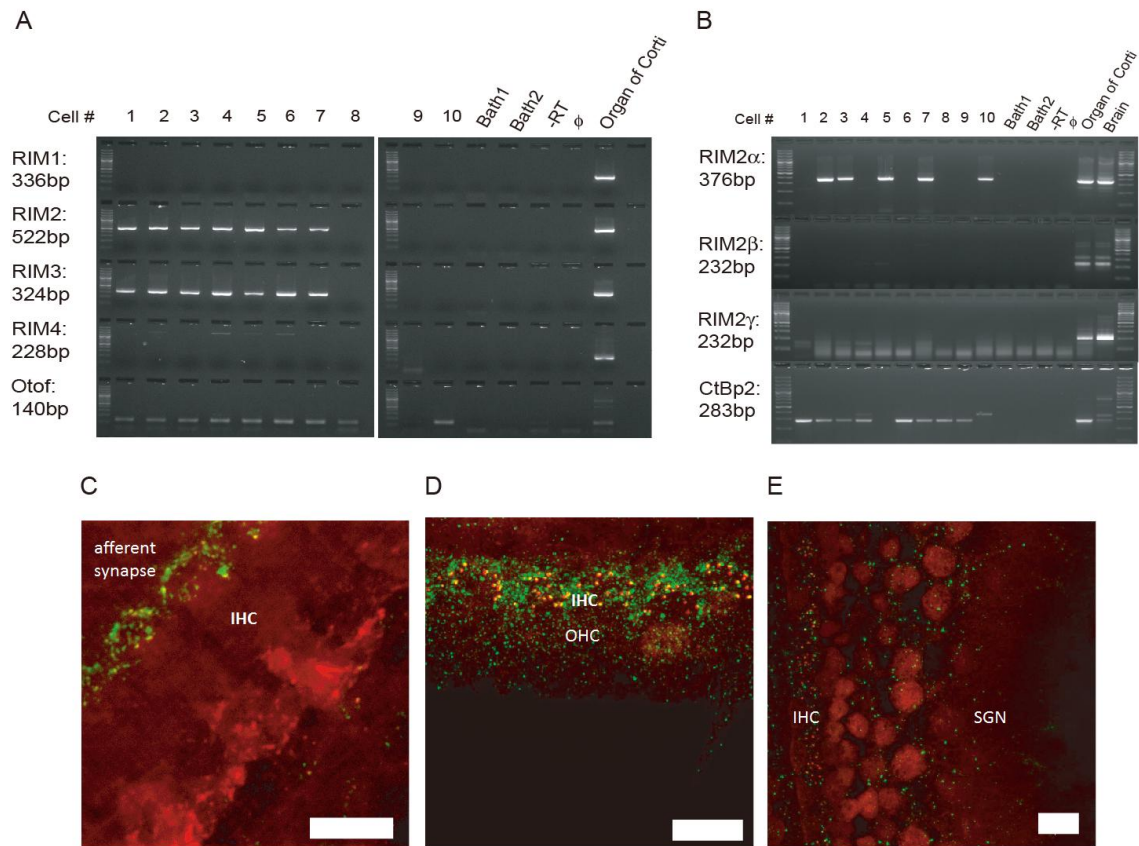


Figure 10 Expression of RIM isoforms at the IHC ribbon synapse in hearing mice

Expressions of RIM isoforms were detected by single cell nested RT-PCR (A and B) and immunohistochemistry (C, D, and E). (A) Expression of RIM isoforms in the C57BL/6 mouse after the hearing onset by single cell nested RT-PCR. Expected sizes of the PCR products are 336 bp for RIM1, 522 bp for RIM2, 324 bp for RIM3, 228 bp for RIM4, and 140 bp for Otoferlin, respectively. Otoferlin was used as a positive control. (B) Expressions of the RIM2 isoforms in IHCs of C57BL/6 mice. Only RIM2 α was detected in IHCs of C57BL/6 mice by single cell nested RT-PCR. The expected size of the PCR products are 376 bp for RIM2 α , 232 bp for RIM2 β , 232 bp for RIM2 γ , and 283 bp for CtBP2, respectively. PCR results were confirmed by sequencing. (C) Projection of confocal sections of C57BL/6 organ of Corti at P8. IHCs were immuno-labeled for ribbons (anti-CtBP2, red) and RIM2 (green). (D) Projection of confocal sections of C57BL/6 organ of Corti at P14. IHCs were immuno-labeled for ribbons (anti-CtBP2, red) and RIM2 (green). (E) Projection of confocal sections of

Results

C57BL/6 organ of Corti at P14, C57BL/6. IHCs were immuno-labeled for ribbons (anti-CtBP2, red) and RIM3 γ (green). Scale bar in C-E: 10 μ m.

Results

3.1.2 Disruption of RIM2 α reduces presynaptic Ca²⁺ currents and exocytic membrane capacitance change

To probe the function of RIM2 α in the IHCs, I next performed perforated patch-clamp recordings on IHCs in RIM2 α knockout (*RIM2 α ^{-/-}*) mice and wild-type littermates (*RIM2 α ^{+/+}*). The mean peak amplitude of the Ca²⁺ current was significantly smaller in *RIM2 α ^{-/-}* IHCs (-105.7 ± 14.8 pA, $n = 5$) than in *RIM2 α ^{+/+}* IHCs (-157.2 ± 15.3 pA, $n = 5$, $p < 0.05$, Figure 11A&B). This can result either from a reduced number of Ca²⁺ channels or a reduced opening probability of Ca²⁺ channels.

The exocytic membrane capacitance change (ΔC_m) evoked by 100 ms-long depolarizations, which is thought to reflect the number of synaptic vesicles fused during synchronous and sustained exocytosis, was also smaller in *RIM2 α ^{-/-}* IHCs (Figure 11C, D, 42.8 ± 14.3 fF, $n = 5$) than that in *RIM2 α ^{+/+}* IHCs (96.3 ± 17.6 fF, $n = 5$, $p < 0.05$).

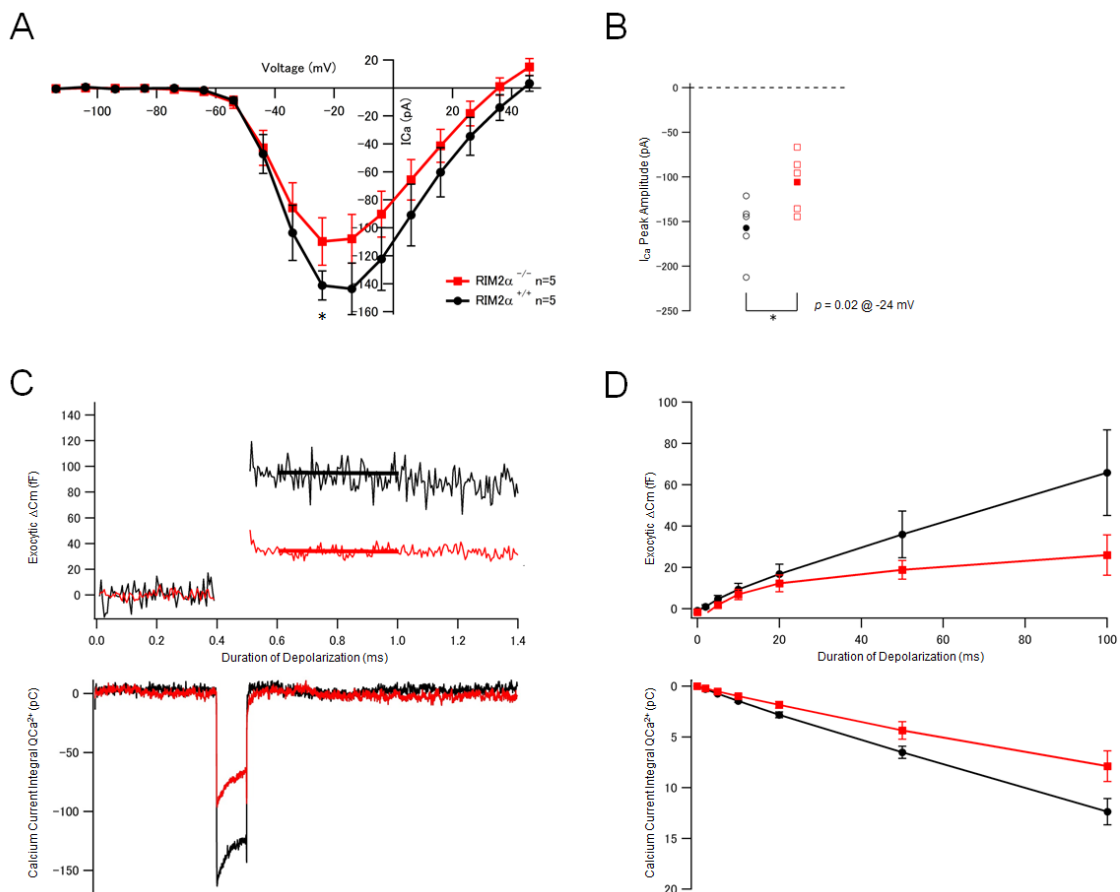


Figure 11 Patch-clamp analysis of presynaptic function of RIM2 α -deficient IHCs

Results

In vitro perforated patch-clamp recording in *RIM2* $\alpha^{+/+}$ (black) and *RIM2* $\alpha^{-/-}$ (red) IHCs. All recording were done with P14-17 mice in the extracellular presence of 2 mM Ca^{2+} .

(A) Current-voltage relationship of *RIM2* $\alpha^{+/+}$ and *RIM2* $\alpha^{-/-}$ obtained from the initial 2-5 ms during 10 ms depolarizations.

(B) The peak amplitude of presynaptic Ca^{2+} currents (I_{Ca}) elicited by depolarization to -24 mV for *RIM2* $\alpha^{+/+}$ and *RIM2* $\alpha^{-/-}$. Individual data points (open circles) and their averages (filled circles) are shown. Mean I_{Ca} peak amplitude was -157.17 ± 15.26 pA in *RIM2* $\alpha^{+/+}$ ($n = 5$), -105.66 ± 14.84 pA in *RIM2* $\alpha^{-/-}$ ($n = 5$). $*p = 0.02$.

(C) Sample traces of I_{Ca} and exocytic capacitance jump (ΔC_m) at 100 ms depolarization in *RIM2* $\alpha^{+/+}$ and *RIM2* $\alpha^{-/-}$, lines indicate the average C_m before and after the depolarization

(D) Summary of integral of Ca^{2+} current (Q_{Ca}) and ΔC_m for depolarizing pulses of various durations. In *RIM2* $\alpha^{-/-}$, both Q_{Ca} and ΔC_m were significantly reduced compared to *RIM2* $\alpha^{+/+}$. ($p < 0.05$).

I analyzed the responses to depolarizations of different durations (Figure 11D) to further investigate the defect of exocytosis and fitted the cumulative exocytosis-time function by the sum of an exponential (raised to a power to accommodate the supralinear rise) and a linear term (Figure 12A). The size of the RRP was approximated as the amplitude of the initial exponential term (fast component), while sustained exocytosis was quantified as the slow linear term (slow component). The RRP size and kinetics of RRP fusion were not significantly different between IHCs of both genotypes (Figure 12B), arguing against a substantial role of *RIM2* α for establishing/stabilizing vesicular release sites and their close spatial coupling to Ca^{2+} channels at IHC active zones. However, the sustained exocytosis rate was reduced from 730 ± 145 fF/sec for *RIM2* $\alpha^{+/+}$ IHCs to 155 ± 101 fF/sec for *RIM2* $\alpha^{-/-}$ IHCs ($p < 0.05$). This result indicated that *RIM2* α is essential for synaptic vesicle replenishment at the IHC ribbon synapse.

Results

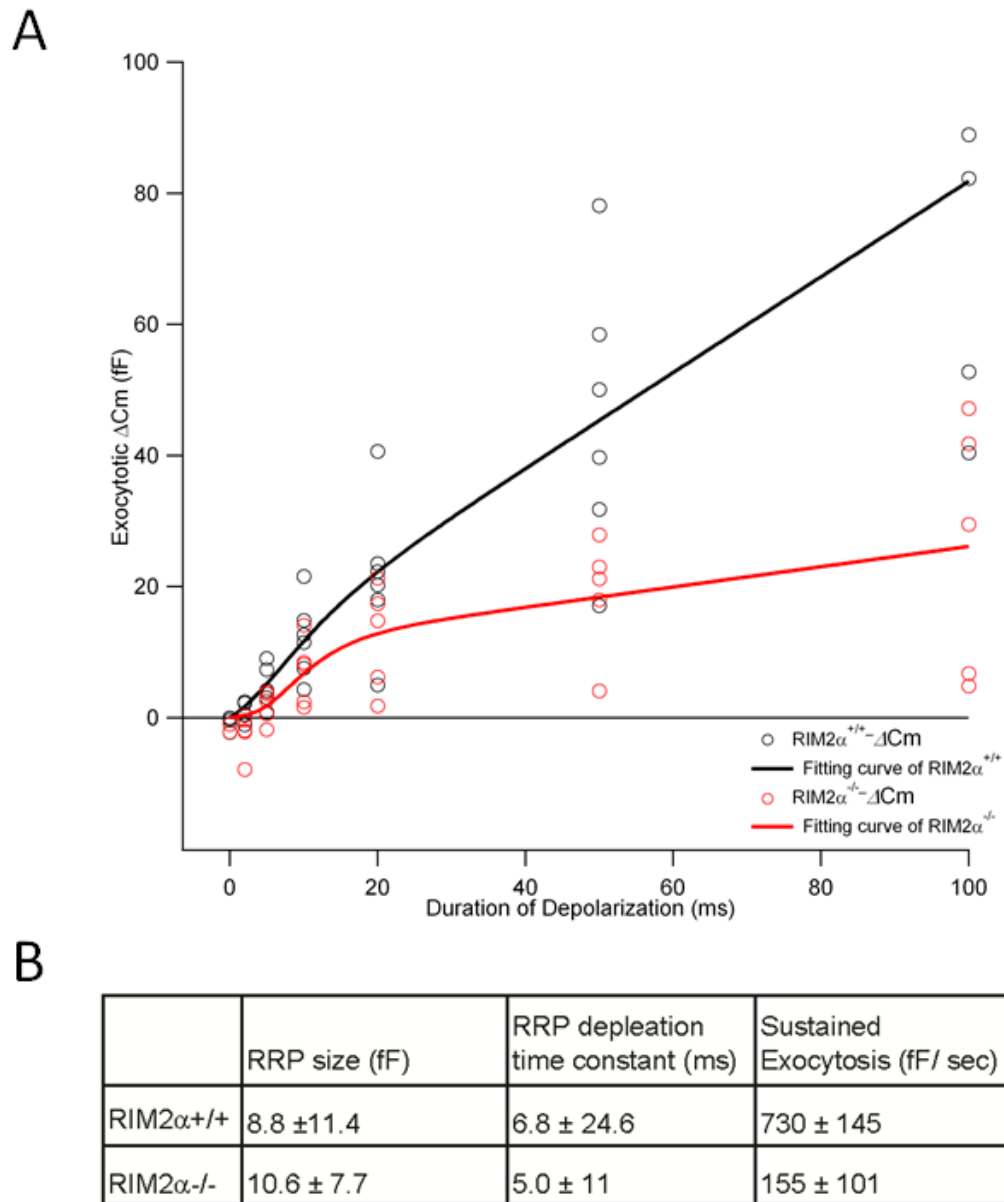


Figure 12 Estimation of vesicle pool size and dynamics

(A) Fitting of ΔC_m (t) relationship using the following function: for estimation of RRP size, RRP depletion time constant and sustained exocytosis rate. Individual data points represent averages for each cell.

(B) The table for values obtained from fitting of ΔC_m (t). Means \pm SEMs are shown.

Results

3.1.3 Auditory systems consequences of the disruption of RIM2 α

Finally, we tested the hearing capability of *RIM2 α ^{-/-}* mice by measuring auditory brainstem responses (ABRs). Mice were anesthetized intraperitoneally with either ketamine plus xylazine or urethane plus xylazine, and the data was pooled because no significant difference in ABR thresholds was detected between ketamine/xylazine anesthetized group and urethane/xylazine anesthetized group. In ABR the first wave (wave I) is a representation of the compound action potential in the spiral ganglion neurons. Then the wave II is primarily generated by glubular cells in the cochlear nucleus (CN). The wave III is partly generated by spherical cells in the CN and partly by their targeting cells. The waves IV and V are generated by MSO principal neurons. (Melcher JR and Kiang NY. 1996c). Despite of unaltered amplitude of waves that were elicited by suprathreshold stimuli (Figure 13A), *RIM2 α ^{-/-}* mice showed higher thresholds than *RIM2 α ^{+/+}* mice at all frequencies examined (Figure 13B) as well as prolonged latencies to peaks of individual waves except for wave I (Figure 13C). DPOAE, which the active amplification by OHCs yields, were normally detected in *RIM2 α ^{-/-}* IHCs (Figure 13D). These results suggest that RIM2 α is necessary for normal hearing, but it is currently unclear whether or how much it can be attributed to the presynaptic deficit observed in IHCs *in vitro*, since neither amplitude nor latency of wave I was significantly altered in *RIM2 α ^{-/-}* mice. Altered synaptic transmission in the auditory brainstem might predominantly underlie the threshold shift observed in *RIM2 α ^{-/-}* mice.

Results

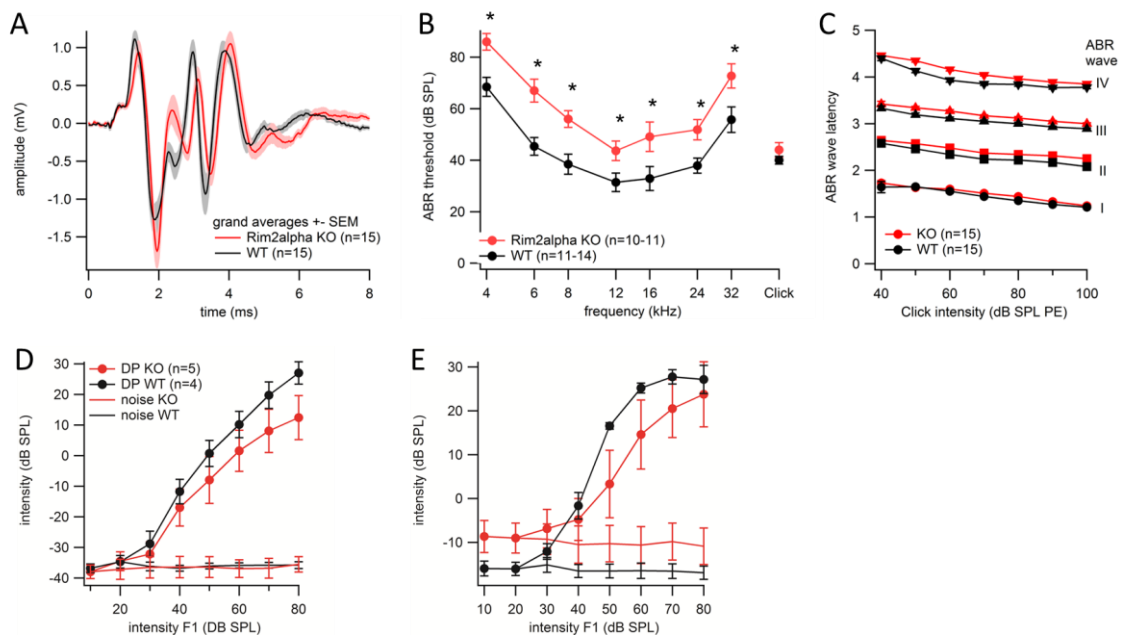


Figure 13 The auditory brainstem response and the distortion product of otoacoustic emission from $RIM2\alpha$ knockout mice

- (A) Auditory brainstem response (ABR) evoked by 80 dB clicks in $RIM2\alpha^{+/+}$ (black) and $RIM2\alpha^{-/-}$ (red) mice.
- (B) ABR audiograms obtained by tone burst or click stimulation in $RIM2\alpha^{+/+}$ and $RIM2\alpha^{-/-}$ mice. Asterisks (*) show significant difference ($p < 0.05$).
- (C) Latency to peak of the each wave at various sound pressure levels. $RIM2\alpha^{-/-}$ mice showed significantly longer latencies to wave peak in all waves except for wave I.
- (D, E) Input-output relationship of DPOAE at 12 kHz (D) and 16 kHz (E) tone bursts derived from $RIM2\alpha^{+/+}$ and $RIM2\alpha^{-/-}$ mice. No significant difference.

3.2 Probing presynaptic function of clarin-1 at the IHC ribbon synapse

The elevated ABR thresholds in clarin-1 knockout ($Clrn1^{-/-}$) mice shown by a previous study (Geng et al., 2009) and reports on a presumptive IHC synaptic phenotype in $Clrn1^{-/-}$ mice (Bitner-Glindzicz et al., 2000; Zallochi et al., 2009) motivated our investigation of their presynaptic function in IHCs. Our collaborators in parallel studied

Results

mechanoelectrical transduction at hair bundles and assessed the number of ribbon synapses (Geng et al., 2012). I explored the physiological impact of the null mutation in clarin-1 on exocytic membrane capacitance changes (ΔC_m) in response to Ca^{2+} currents (I_{Ca}) evoked by step depolarizations by perforated-patch recordings from IHCs in hearing mice (P14-20). I found that neither the integral of $Ca_v1.3$ -mediated Ca^{2+} currents upon depolarization nor corresponding ΔC_m was different between $Clrn1^{-/-}$ and $Clrn1^{+/+}$ IHCs (Figure 14C). In summary, $Clrn1^{-/-}$ IHCs showed normal I_{Ca} and ΔC_m in response to hair cell depolarizations. These results argue against an essential function of clarin-1 at the IHC ribbon synapse.

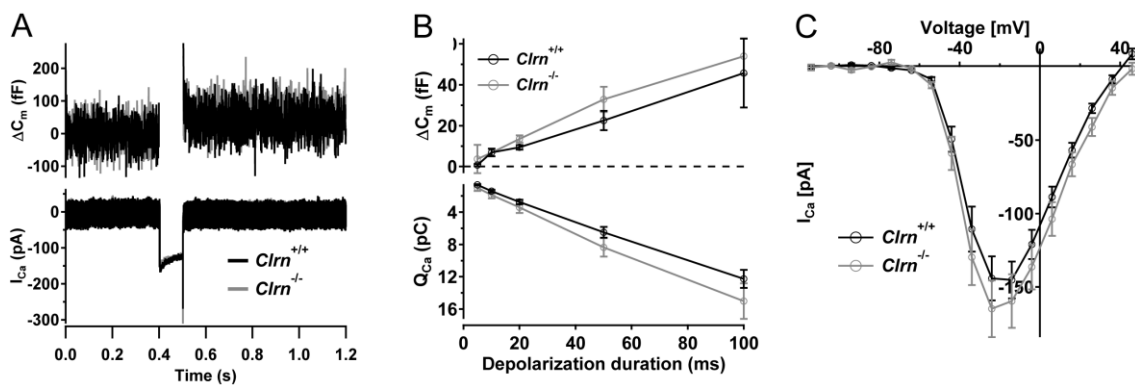


Figure 14 Patch-clamp analysis of presynaptic function of clarin-1 at the IHC ribbon synapse

(A) Representative exocytic membrane capacitance changes (ΔC_m , top) and Ca^{2+} currents (I_{Ca} , bottom) in response to 50 ms depolarization from a resting potential of -84 mV to -14 mV in $Clrn1^{-/-}$ (grey) and $Clrn1^{+/+}$ (black) IHCs.

(B) Grand average ΔC_m and Q_{Ca} for step depolarizations to 14 mV of variable durations. All responses are given as grand averages (calculated from the means of the individual cells) \pm SEM.

(C) Current-voltage relationship for $Ca_v1.3$ Ba^{2+} currents in control (black, $n=12$ IHCs) and mutant ($n=10$ IHCs) IHCs. Currents were evoked by 10 ms step depolarizations from a resting potential of -84 mV to variable potentials and their peak current was plotted against test potential.

4. Discussion

4.1 RIM2 α regulates L-type Ca²⁺ current and Ca²⁺-triggered exocytosis at the IHC ribbon synapse

I demonstrated that the IHCs of hearing mice express RIM2 α and RIM3 γ , but not other isoforms of RIMs, at their active zones and that RIM2 α plays a regulatory role in synaptic transmission at the IHC ribbon synapse. This study, for the first time, demonstrates functional roles of RIM2 α , after previous studies failed to assign any roles to it (Schoch et al., 2006). Strikingly, the IHC ribbon synapse and central synapses do not share common isoform(s) of α -RIMs to control Ca²⁺-triggered release, presumably due to their different origins (sensory epithelium versus neuron). This is in line with other previous findings, which show that the IHC ribbon synapse differs from other synapses in some respects. In addition to using Cav1.3 L-type Ca²⁺ channels for secretion control, the IHCs likely utilize Otoferlin instead of the conventional Ca²⁺ sensor synaptotagmins to mediate Ca²⁺-regulated vesicle fusion (Roux et al., 2006) and vesicle replenishment (Pangršič et al., 2010). Moreover, the IHC ribbon synapse seems to operate without neuronal SNARE proteins (Nouvian et al., 2011). Thus, the IHC ribbon synapse operates in a specialized manner so that it can keep pace with submillisecond-order stimuli, in order to perform fast and faithful sound encoding (for review, see Pangršič et al., 2012).

Previous work studied the functions of RIMs at conventional active zones using conventional or conditional knockout mouse lines. At the hippocampal CA3-CA1 synapse of RIM1 α knockout mice, Ca²⁺-triggered release was reduced (Calakos et al., 2004) and short-term synaptic plasticity was altered (Schoch et al., 2002). Deletion of RIM1 α reduced release probability in excitatory synapses in the amygdala (Fourcaudot et al., 2008) just like it did in the inhibitory synapses in the hippocampus (Kaeser et al., 2008a). In the absence of RIM1 α , LTP was abolished in the excitatory synapses in the hippocampus (Castillo et al., 2002; Huang et al., 2005; Pelkey and McBain, 2008) and the cerebellum (Castillo et al., 2002; Lonart et al., 2003; Simsek-Duran et al., 2004) as well as it was in the inhibitory synapses in the cerebellum (Lachamp et al., 2009). LTD was also abolished in inhibitory synapses in the hippocampus and the amygdala

Discussion

(Chevaleyre et al., 2007). Kaeser et al. (2008a) showed that double-knockout of RIM1 α and RIM1 β reduced release probability in the CA3-CA1 synapse and further abolished LTP in the DG-CA3 synapse and LTD in the inhibitory interneuron synapses of the hippocampus. Moreover, double-knockout of RIM1 α and RIM2 α reduced the amplitude and increased failure rate of evoked release at the embryonic neuromuscular junction (Schoch et al., 2006). Furthermore, conditional double knockout of RIM1 α and RIM2 α disrupted synaptic transmission by decreasing Ca²⁺ channel density and number of docked and readily releasable vesicles at the active zone of the calyx of Held synapse in the auditory brainstem (Han et al., 2011). As already stated, knockout of RIM2 α alone caused no synaptic deficits (Schoch et al., 2006).

In this study, however, I demonstrated that RIM2 α , as a key player, regulates the Ca_v1.3-mediated Ca²⁺ current and synaptic vesicle replenishment at the IHC ribbon synapse (Figure 15). I postulate that the reduced Ca_v1.3 Ca²⁺ current reflects a reduction in the number of Ca²⁺ channels, which also impairs synaptic Ca²⁺ influx. This is consistent with findings at the calyx of Held (Han et al., 2011) and excitatory synapses of hippocampal neurons in culture (Kaeser et al., 2011). While not yet tested by electron microscopy, I conclude from the unaltered RRP size that the number of membrane-proximal vesicles is not changed in the absence of RIM2 α . Thereby the IHC afferent synapse deviates from the calyx of Held synapse, which showed a reduced RRP in the absence of α -RIMs (Han et al., 2011). Moreover, my finding of an impaired vesicle replenishment reports a yet unknown RIM function.

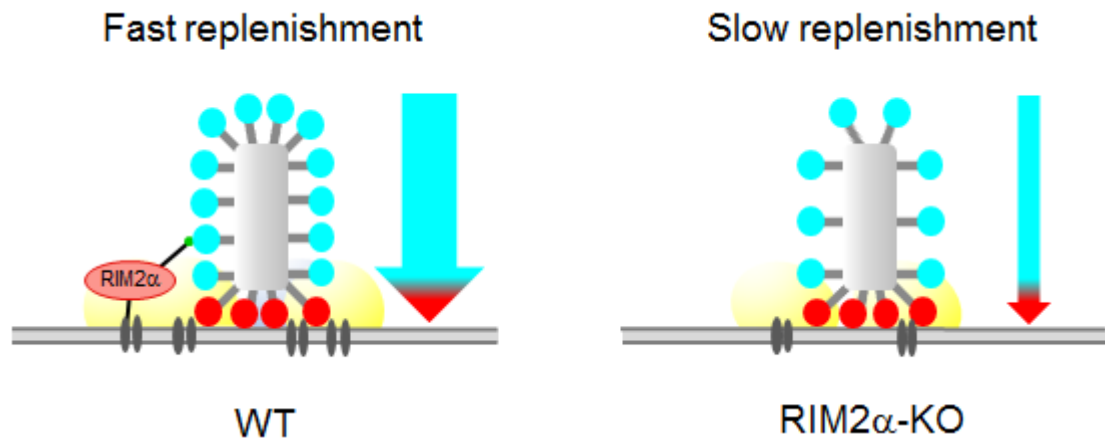


Figure 15 Schematic representation of putative functions of RIM2 α at the IHC ribbon synapse

Membrane-associated vesicles (red), ribbon tethered vesicles (blue) are shown. The width of arrows indicates the rate of synaptic vesicle replenishment. It is postulated that RIM2 α -knockout IHCs show a normal number of membrane-associated vesicles, but reduced density of Ca_v1.3-type Ca²⁺ channels (black) and slower replenishment of synaptic vesicles (arrows). Yellow clouds around the Ca²⁺ channels shows Ca²⁺ nanodomains for triggering synaptic vesicle fusion. RIM2 α might interact with Ca_v1.3-type Ca²⁺ channels as well as synaptic vesicles via Rab3 (green).

4.2 Discrepancy between the *in vitro* finding of impaired vesicle replenishment with reduced Ca²⁺ currents and the *in vivo* finding of relatively intact auditory brainstem responses

Table 3 is a summary of the exocytic parameters obtained by presynaptic capacitance recordings from IHCs in RIM2 α knockout mice, Bassoon mutant mice with a deletion of exon 4/5 (*BSN* ^{Δ Ex4/5}, Khimich et al., 2005), and Otoferlin mutant mice with a single amino acid substitution of D1767G in the C₂F domain (*Pachanga*, Pangršič et al., 2010).

Discussion

	RRP size (fF)	RRP depletion time constant (ms)	Sustained exocytosis (fF/sec)	Ref
<i>RIM2α</i> ^{+/+}	8.8	6.8	730	this study
<i>RIM2α</i> ^{-/-}	10.6	5.0	155	
<hr/>				
<i>BSN</i> ^{wt}	15-18	8-9	265	Khimich et al., 2005
<i>BSN</i> ^{ΔEx4/5}	5	11	?	
<hr/>				
<i>Otof</i> ^{+/+}	7.0	5.2	391	Pangršič et al., 2010
<i>Otof</i> ^{Pga/Pga}	9.4	3.9	98	

Table 3 Quantification of exocytosis in *RIM2α*, Bassoon, and Otoferlin mutant IHCs

The *RIM2α*^{-/-} and *Otof*^{Pga/Pga} IHCs share a common phenotype of slower sustained exocytosis with intact RRP size and RRP depletion rate. The slower sustained rate in both mutants is compatible with their roles in synaptic vesicle replenishment potentially related to priming or active zone clearance. The intact RRP size and RRP depletion time constant in the *RIM2α*^{-/-} IHCs suggest that *RIM2α* is not essential for docking and fusion of synaptic vesicles at the active zones of IHC ribbon synapse. In contrast, the *BSN*^{ΔEx4/5} IHCs have a unique phenotype of reduced synaptic complement of Ca²⁺ channels, fewer docked vesicles resulting in a reduced RRP size and slower sustained exocytosis (Khimich et al., 2005; Frank et al., 2010). Finding impaired sustained exocytosis in *RIM2α* and otoferlin mutants is interesting also because those mice show very different hearing. While ABRs are relatively maintained in *RIM2α*^{-/-}, the *Pachanga* mice essentially lack ABRs. The difference could be a quantitative one: the rate of sustained exocytosis of *RIM2α*^{-/-} IHCs was almost twice as high as in the *Pachanga* IHCs. This might be caused by higher probability of spike generation in the type I spiral ganglion neurons at the *RIM2α*^{-/-} IHC afferent synapse due to following mechanisms: down-regulated K⁺ channels leads enhanced excitability of afferent

Discussion

dendrites, and/or impaired developmental pruning of synaptic contacts (for review, see Bulankina et al., 2012). Additional works on single auditory nerve fiber responses and synaptic ultrastructure in $RIM2\alpha^{-/-}$ will be needed to further clarify the issue.

Finally, a recent study has shown that γ -RIMs are expressed in a variety of neurons in the cortex, cerebellum, olfactory bulb, and retina. Remarkably, $RIM3\gamma$, but not $RIM4\gamma$, exhibits a synaptic expression pattern. In contrast, $RIM4\gamma$ is ubiquitously expressed along axons and dendrites. Despite the differential localization, either of them controls the neuronal branching. With regard to the synaptic function of γ -RIMs, their knock-down decreases miniature EPSC amplitude recorded from primary cortical neurons (Fuentes, 2010). Thus, γ -RIMS might play substantial roles at other synapses including the cochlear hair cell synapses. However, further insight into the function of γ -RIMs at the IHC ribbon synapse is out of scope of the current study.

4.3 Clarin-1 is dispensable for the ribbon synapse development and function

In the present study, I provided evidence against a function of clarin-1 at the IHC ribbon synapse in hearing mice. Although previous studies predicted its involvement in hair cell synapse function (Adato et al., 2002, Geng et al., 2009, Zallocchi et al., 2009 and 2012), I found no evidence of synaptic dysfunction in the absence of clarin-1. The $Clrn1^{-/-}$ mouse cochlea (Zallocchi et al., 2012) exhibited no morphological changes in the development of the IHC ribbon synapse (present study). Moreover, $Clrn1^{-/-}$ IHCs did not show larger Ca^{2+} currents than wild-type controls, which was observed in athyroid IHCs at the same age (Sendin et al., 2007). These results further argue against a potential role of clarin-1 in the ribbon synapse development. Besides, a recent study ruled out an involvement of clarin-1 in photoreceptor function (Geller et al., 2009). Taken together, these sets of evidence suggest that clarin-1 is dispensable for ribbon synapse development and function.

In contrast, our collaborators have shown that clarin-1 is indispensable for development or maintenance of the hair bundles (Geng et al., 2012), as was indicated by preceding studies (Geng et al., 2009; Tian et al., 2009). The reduced amplitude of MET channel-mediated currents due to the disrupted hair bundles in $Clrn1^{-/-}$ mice likely

Discussion

underlies elevated thresholds and delayed latencies of peaks in ABRs. Thus, hearing loss in the USH type III mouse model is caused by a hair bundle deficit.

The cochlear implant, the only treatment for USH at present, showed satisfying outcomes in Finnish USH3 patients (Pietola et al., 2012). This also supports the fact that USH3 patients have no major synaptic deficits in the auditory ascending pathways after the SGNs, which the electrodes directly stimulate. Restoration of hair bundle function by gene therapy in USH3 patients would promise faithful sound encoding through the intact IHC ribbon synapse.

References

5. References

- Adato A, Kalinski H, Weil D, Chaib H, Korostishevsky M, Bonne-Tamir B (1999) Possible interaction between USH1B and USH3 gene products as implied by apparent digenic deafness inheritance. *Am J Hum Genet* 65:261-265.
- Adato A, Vreugde S, Joensuu T, Avidan N, Hamalainen R, Belenkiy O, Olender T, Bonne-Tamir B, Ben-Asher E, Espinos C, Millán JM, Lehesjoki AE, Flannery JG, Avraham KB, Pietrokovski S, Sankila EM, Beckmann JS, Lancet D (2002) USH3A transcripts encode clarin-1, a four-transmembrane domain protein with a possible role in sensory synapses. *Eur J Hum Genet* 10:339-350.
- Ahmed ZM, Riazuddin S, Bernstein SL, Ahmed Z, Khan S, Griffith AJ, Morell RJ, Friedman TB, Riazuddin S, Wilcox ER (2001) Mutations of the protocadherin gene PCDH15 cause Usher syndrome type 1F. *Am J Hum Genet* 69:5–34.
- Alagramam KN, Yuan H, Kuehn MH, Murcia CL, Wayne S, Srisailpathy CR, Lowry RB, Knaus R, Van Laer L, Bernier FP, Schwartz S, Lee C, Morton CC, Mullins RF, Ramesh A, Van Camp G, Hageman GS, Woychik RP, Smith RJ (2001) Mutations in the novel protocadherin PCDH15 cause Usher syndrome type 1F. *Hum Mol Genet* 10:1709-1718.
- Aller E, Jaijo T, Oltra S, Alió J, Galán F, Nájera C, Beneyto M, Millán JM (2004) Mutation screening of USH3 gene (clarin-1) in Spanish patients with Usher syndrome: low prevalence and phenotypic variability. *Clin Genet* 66:525-529.
- Baig SM, Koschak A, Lieb A, Gebhart M, Dafinger C, Nürnberg G, Ali A, Ahmad I, Sinnegger-Brauns MJ, Brandt N, Engel J, Mangoni ME, Farooq M, Khan HU, Nürnberg P, Striessnig J, Bolz HJ (2011) Loss of Ca(v)1.3 (CACNA1D) function in a human channelopathy with bradycardia and congenital deafness. *Nat Neurosci* 14:77-84.
- Bitner-Glindzicz M, Lindley KJ, Rutland P, Blaydon D, Smith VV, Milla PJ, Hussain K, Furth-Lavi J, Cosgrove KE, Shepherd RM, Barnes PD, O'Brien RE, Farndon PA, Sowden J, Liu XZ, Scanlan MJ, Malcolm S, Dunne MJ, Aynsley-Green A, Glaser B (2000) A recessive contiguous gene deletion causing infantile hyperinsulinism, enteropathy and deafness identifies the Usher type 1C gene. *Nat Genet* 26:56-60.

References

- Blunkina AV, Moset T (2012) Neural circuit development in the mammalian cochlea. *Physiology (Bethesda)* 27:100112.
- Bolz H, von Brederlow B, Ramírez A, Bryda EC, Kutsche K, Nothwang HG, Seeliger M, del C-Salcedó Cabrera M, Vila MC, Molina OP, Gal A, Kubisch C (2001) Mutation of CDH23, encoding a new member of the cadherin gene family, causes Usher syndrome type 1D. *Nat Genet* 27:108-112.
- Bork JM, Peters LM, Riazuddin S, Bernstein SL, Ahmed ZM, Ness SL, Polomeno R, Ramesh A, Schloss M, Srisailpathy CR, Wayne S, Bellman S, Desmukh D, Ahmed Z, Khan SN, Kaloustian VM, Li XC, Lalwani A, Riazuddin S, Bitner-Glindzicz M, Nance WE, Liu XZ, Wistow G, Smith RJ, Griffith AJ, Wilcox ER, Friedman TB, Morell RJ (2001) Usher syndrome 1D and nonsyndromic autosomal recessive deafness DFNB12 are caused by allelic mutations of the novel cadherin-like gene CDH23. *Am J Hum Genet* 68:26-37.
- Brand A, Behrend O, Marquardt T, McAlpine D, Grothe B (2002) Precise inhibition is essential for microsecond interaural time difference coding. *Nature* 417:502-503.
- Brandt A, Striessnig J, Moser T (2003) Ca_v1.3 channels are essential for development and presynaptic activity of cochlear inner hair cells. *J Neurosci* 23:10832–10840.
- Brandt A, Khimich D, Moser T (2005) Few Ca_v1.3 channels regulate the exocytosis of a synaptic vesicle at the hair cell ribbon synapse. *J Neurosci* 25:11577-11585.
- Brown SD, Hardisty-Hughes RE, Mburu P (2008) Quiet as a mouse: dissecting the molecular and genetic basis of hearing. *Nat Rev Genet* 9:277-290.
- Bunt AH (1971) Enzymatic digestion of synaptic ribbons in amphibian retinal photoreceptors. *Brain Res* 25:571-577.
- Calakos N, Schoch S, Südhof TC, Malenka RC (2004) Multiple roles for the active zone protein RIM1 α in late stages of neurotransmitter release. *Neuron* 42:889-896.
- Castillo PE, Schoch S, Schmitz F, Südhof TC, Malenka RC (2002). RIM1 α is required for presynaptic long-term potentiation. *Nature* 415:327-330.
- Chaïb H, Kaplan J, Gerber S, Vincent C, Ayadi H, Slim R, Munnich A, Weissenbach J, Petit C (1997) A newly identified locus for Usher syndrome type I, USH1E, maps to chromosome 21q21. *Hum Mol Genet* 6:27-31.

References

- Chevalleyre V, Heifets BD, Kaeser P, Südhof TC, Purpura DP, Castillo PE (2007) Endocannabinoid-mediated longterm plasticity requires cAMP/PKA signaling and RIM1 α . *Neuron* 54:801-812.
- Chien W, Lee DJ (2010) Physiology of the auditory system. In: Cummings Otolaryngology Head & Neck Surgery 5th Edition, pp1838-1849. Mosby.
- Cui G, Meyer AC, Calin-Jageman I, Neef J, Haeseleer F, Moser T, Lee A. Ca²⁺-binding proteins tune Ca²⁺-feedback to Cav1.3 channels in mouse auditory hair cells. *J Physiol* 585:791-803.
- Dallos P, Fakler B (2002) Prestin, a new type of motor protein. *Nat Rev Mol Cell Biol* 3:104-111.
- Darrow KN, Simons EJ, Dodds L, Liberman MC (2006) Dopaminergic innervation of the mouse inner ear: evidence for a separate cytochemical group of cochlear efferent fibers. *J Comp Neurol* 498:403-414.
- Dick O, Hack I, Altmann WD, Garner CC, Gundelfinger ED, Brandstätter JH (2001) Localization of the presynaptic cytomatrix protein Piccolo at ribbon and conventional synapses in the rat retina: comparison with Bassoon. *J Comp Neurol* 439:224-234.
- Dick O, tom Dieck S, Altmann WD, Ammermüller J, Weiler R, Garner CC, Gundelfinger ED, Brandstätter JH (2003) The presynaptic active zone protein bassoon is essential for photoreceptor ribbon synapse formation in the retina. *Neuron* 37:775-786.
- Ebermann I, Scholl HP, Charbel Issa P, Becirovic E, Lamprecht J, Jurklics B, Millán JM, Aller E, Mitter D, Bolz H (2007) A novel gene for Usher syndrome type 2: mutations in the long isoform of whirlin are associated with retinitis pigmentosa and sensorineural hearing loss. *Hum Genet* 121:203-211.
- Ebermann I, Phillips JB, Liebau MC, Koenekoop RK, Schermer B, Lopez I, Schäfer E, Roux AF, Dafinger C, Bernd A, Zrenner E, Claustres M, Blanco B, Nürnberg G, Nürnberg P, Ruland R, Westerfield M, Benzing T, Bolz HJ (2010) PDZD7 is a modifier of retinal disease and a contributor to digenic Usher syndrome. *J Clin Invest* 120:1812-23.

References

- Elgoyhen AB, Johnson DS, Boulter J, Vetter DE, Heinemann S (1994) Alpha 9: an acetylcholine receptor with novel pharmacological properties expressed in rat cochlear hair cells. *Cell* 79:705-715.
- Eudy JD, Weston MD, Yao S, Hoover DM, Rehm HL, Ma-Edmonds M, Yan D, Ahmad I, Cheng JJ, Ayuso C, Cremers C, Davenport S, Moller C, Talmadge CB, Beisel KW, Tamayo M, Morton CC, Swaroop A, Kimberling WJ, Sumegi J (1998) Mutation of a gene encoding a protein with extracellular matrix motifs in Usher syndrome type IIa. *Science* 280:1753-1757.
- Eybalin M, Charachon G, Renard N (1993) Dopaminergic lateral efferent innervation of the guinea-pig cochlea: immunoelectron microscopy of catecholamine-synthesizing enzymes and effect of 6-hydroxydopamine. *Neuroscience* 54:133-142.
- Fields RR, Zhou G, Huang D, Davis JR, Möller C, Jacobson SG, Kimberling WJ, Sumegi J (2002) Usher syndrome type III: revised genomic structure of the USH3 gene and identification of novel mutations. *Am J Hum Genet* 71:607-617.
- Fourcaudot E, Gambino F, Humeau Y, Casassus G, Shaban H, Poulain B, Luthi A (2008) cAMP/PKA signaling and RIM1a mediate presynaptic LTP in the lateral amygdala. *Proc Natl Acad Sci U S A* 105:15130-15135.
- Frank T, Rutherford MA, Strenzke N, Neef A, Pangršič T, Khimich D, Fejtova A, Gundelfinger ED, Liberman MC, Harke B, Bryan KE, Lee A, Egner A, Riedel D, Moser T (2010) Bassoon and the synaptic ribbon organize Ca²⁺ channels and vesicles to add release sites and promote refilling. *Neuron* 68:724-738.
- Fuchs PA, Glowatzki E, Moser T (2003) The afferent synapse of cochlear hair cells. *Curr Opin Neurobiol* 13:452-458.
- Fuchs PA, Murrow BW (1992) Cholinergic inhibition of short (outer) hair cells of the chick's cochlea. *J Neurosci* 12:800-809.
- Fuentes EAB (2010) Localization and functional role of RIM3 γ and RIM4 γ , the small members of the RIM protein family. PhD Thesis, University of Bonn, Bonn, Germany.

References

- Gebhart M, Juhasz-Vedres G, Zuccotti A, Brandt N, Engel J, Trockenbacher A, Kaur G, Obermair GJ, Knipper M, Koschak A, Striessnig J (2010) Modulation of Cav1.3 Ca²⁺ channel gating by Rab3 interacting molecule. *Mol Cell Neurosci* 44:246-259.
- Geng R, Geller SF, Hayashi T, Ray CA, Reh TA, Bermingham-McDonogh O, Jones SM, Wright CG, Melki S, Imanishi Y, Palczewski K, Alagramam KN, Flannery JG (2009) Usher syndrome IIIA gene clarin-1 is essential for hair cell function and associated neural activation. *Hum Mol Genet* 18:2748-2760.
- Geng R, Melki S, Chen D, Tian G, Furness D, Oshima-Takago T, Neef J, Moser T, Askew C, Horwitz G, Holt J, Imanishi Y, Alagramam KN (2012) The Mechanosensory Structure of the Hair Cell Requires Clarin-1, a Protein Encoded by Usher Syndrome III Causative Gene. *J Neurosci* 32:9485-9498.
- Geller SF, Guerin KI, Visel M, Pham A, Lee ES, Dror AA, Avraham KB, Hayashi T, Ray CA, Reh TA, Bermingham-McDonogh O, Triffo WJ, Bao S, Isosomppi J, Västinsalo H, Sankila EM, Flannery JG (2009) CLRN1 is nonessential in the mouse retina but is required for cochlear hair cell development. *PLoS Genet* 5:e1000607.
- Glowatzki E, Fuchs PA (2000) Cholinergic synaptic inhibition of inner hair cells in the neonatal mammalian cochlea. *Science* 288:2366-2368.
- Grant L, Fuchs P (2008) Calcium- and calmodulin-dependent inactivation of calcium channels in inner hair cells of the rat cochlea. *J Neurophysiol* 99:2183-2193.
- Gregory FD, Bryan KE, Pangršič T, Calin-Jageman IE, Moser T, Lee A. (2011) Harmonin inhibits presynaptic Cav1.3 Ca²⁺ channels in mouse inner hair cells. *Nat Neurosci* 14:1109-1111.
- Guinan JJ Jr, Warr WB, Norris BE (1984) Topographic organization of the olivocochlear projections from the lateral and medial zones of the superior olivary complex. *J Comp Neurol* 226:21-27.
- Han Y, Kaeser PS, Südhof TC, Schneggenburger R (2011) RIM determines Ca²⁺ channel density and vesicle docking at the presynaptic active zone. *Neuron* 69:304-16.
- Herrera W, Aleman TS, Cideciyan AV, Roman AJ, Banin E, Ben-Yosef T, Gardner LM, Sumaroka A, Windsor EA, Schwartz SB, Stone EM, Liu XZ, Kimberling WJ,

References

- Jacobson SG (2008) Retinal disease in Usher syndrome III caused by mutations in the clarin-1 gene. *Invest Ophthalmol Vis Sci* 49:2651-2660.
- Hibino H, Nin F, Tsuzuki C, Kurachi Y (2010) How is the highly positive endocochlear potential formed? The specific architecture of the stria vascularis and the roles of the ion-transport apparatus. *Pflugers Arch* 459:521-533.
- Hibino H, Pironkova R, Onwumere O, Vologodskaja M, Hudspeth AJ, Lesage F (2002) RIM binding proteins (RBPs) couple Rab3-interacting molecules (RIMs) to voltage-gated Ca²⁺ channels. *Neuron* 34:411-423.
- Huang YY, Zakharenko SS, Schoch S, Kaeser PS, Janz R, Südhof TC, Siegelbaum SA, Kandel ER (2005) Genetic evidence for a protein-kinase-A-mediated presynaptic component in NMDA-receptor-dependent forms of long-term synaptic potentiation. *Proc Natl Acad Sci U S A* 102:9365-9370.
- Hudspeth A (1997) Mechanical amplification of stimuli by hair cells. *Curr Opin Neurobiol* 7:480-486.
- Joensuu T, Hämäläinen R, Yuan B, Johnson C, Tegelberg S, Gasparini P, Zelante L, Pirvola U, Pakarinen L, Lehesjoki AE, de la Chapelle A, Sankila EM (2001) . Mutations in a novel gene with transmembrane domains underlie Usher syndrome type 3. *Am J Hum Genet* 69:673-684.
- Johnson CP, Chapman ER (2010) Otoferlin is a calcium sensor that directly regulates SNARE-mediated membrane fusion. *J Cell Biol* 191:187-197.
- Kaeser PS, Kwon HB, Chiu CQ, Deng L, Castillo PE, Südhof TC (2008a) RIM1a and RIM1b are synthesized from distinct promoters of the RIM1 gene to mediate differential but overlapping synaptic functions. *J Neurosci* 28:13435-13447.
- Kaeser PS, Deng L, Wang Y, Dulubova I, Liu X, Rizo J, Südhof TC (2011) RIM proteins tether Ca²⁺ channels to presynaptic active zones via a direct PDZ-domain interaction. *Cell* 144:282-295.
- Katz E, Elgoyhen AB, Gómez-Casati ME, Knipper M, Vetter DE, Fuchs PA, Glowatzki E (2004) Developmental regulation of nicotinic synapses on cochlear inner hair cells. *J Neurosci* 24:7814-7820.

References

- Katz PS, Kirk MD, Govind CK (1993) Facilitation and depression at different branches of the same motor axon: evidence for presynaptic differences in release. *J Neurosci* 13:3075-3089.
- Kharkovets T, Dedek K, Maier H, Schweizer M, Khimich D, Nouvian R, Vardanyan V, Leuwer R, Moser T, Jentsch TJ (2006) Mice with altered KCNQ4 K⁺ channels implicate sensory outer hair cells in human progressive deafness. *EMBO J* 25:642-652.
- Khimich D, Nouvian R, Pujol R, Tom Dieck S, Egner A, Gundelfinger ED, Moser T (2005) Hair cell synaptic ribbons are essential for synchronous auditory signalling. *Nature* 434:889-894.
- Kimberling WJ, Weston MD, Möller C, Davenport SL, Shugart YY, Priluck IA, Martini A, Milani M, Smith RJ (1990) Localization of Usher syndrome type II to chromosome 1q. *Genomics* 7:245-249.
- Kong JH, Adelman JP, Fuchs PA (2008) Expression of the SK2 calcium-activated potassium channel is required for cholinergic function in mouse cochlear hair cells. *J Physiol* 586:5471-5485.
- Kremer H, van Wijk E, Märker T, Wolfrum U, Roepman R (2006) Usher syndrome: molecular links of pathogenesis, proteins and pathways. *Hum Mol Genet* 15:262-270.
- Kros CJ, Ruppertsberg JP, Rüscher A (1998) Expression of a potassium current in inner hair cells during development of hearing in mice. *Nature* 394:281-284.
- Kros, CJ (1996) Physiology of mammalian cochlear hair cells. In *Springer Handbook of Auditory Research, Vol. 8: The Cochlea*, ed. Dallos P, Popper AN & Fay RR, p318-385. Springer-Verlag, New York.
- Lachamp PM, Liu Y, Liu SJ (2009) Glutamatergic modulation of cerebellar interneuron activity is mediated by an enhancement of GABA release and requires protein kinase A/RIM1 α signaling. *J Neurosci* 29:381-392.
- Lagnado L (2003) Ribbon synapses. *Curr Biol*. 13:R631.
- Lenzi D, von Gersdorff H (2001) Structure suggests function: the case for synaptic ribbons as exocytotic nanomachines. *Bioessays* 23:831-840.

References

- Liberman MC, Gao J, He DZ, Wu X, Jia S, Zuo J (2002) Prestin is required for electromotility of the outer hair cell and for the cochlear amplifier. *Nature* 419:300-304.
- Lonart G, Schoch S, Kaeser PS, Larkin CJ, Südhof TC, Linden DJ (2003) Phosphorylation of RIM1 α by PKA triggers presynaptic long-term potentiation at cerebellar parallel fiber synapses. *Cell* 115:49-60.
- Magupalli VG, Schwarz K, Alpadi K, Natarajan S, Seigel GM, Schmitz F (2008) Multiple RIBEYE-RIBEYE interactions create a dynamic scaffold for the formation of synaptic ribbons. *J Neurosci* 28:7954-7967.
- Marcotti W, Johnson SL, Holley MC, Kros CJ (2003) Developmental changes in the expression of potassium currents of embryonic, neonatal and mature mouse inner hair cells. *J Physiol* 548:383-400.
- Matthews G, Fuchs P (2010) The diverse roles of ribbon synapses in sensory neurotransmission. *Nat Rev Neurosci* 11:812-822
- Melcher JR, Kiang NY (1996) Generators of the brainstem auditory evoked potential in cat. III: Identified cell populations. *Hear Res.* 93:52-71.
- Meyer AC, Frank T, Khimich D, Hoch G, Riedel D, Chapochnikov NM, Yarin YM, Harke B, Hell SW, Egner A, Moser T (2009) Tuning of synapse number, structure and function in the cochlea. *Nat Neurosci* 12:444-453.
- Mittelstaedt T, Alvarez-Baron E, Schoch S (2010) RIM proteins and their role in synapse function. *Biol Chem* 391:599-606.
- Marcotti W, Johnson SL, Kros CJ (2004) A transiently expressed SK current sustains and modulates action potential activity in immature mouse inner hair cells. *J Physiol* 560:691-708.
- Moser T, Beutner D (2000) Kinetics of exocytosis and endocytosis at the cochlear inner hair cell afferent synapse of the mouse. *Proc Natl Acad Sci U S A* 97:883-888.
- Moser T, Brandt A, Lysakowski A (2006) Hair cell ribbon synapses. *Cell Tissue Res* 326:347-359.
- Moser T, Neef A, Khimich D (2006) Mechanisms underlying the temporal precision of sound coding at the inner hair cell ribbon synapse. *J Physiol* 576:55-62.

References

- Müller U (2008) Cadherins and mechanotransduction by hair cells. *Curr Opin Cell Biol* 20:557-566.
- Mustapha M, Chouery E, Torchard-Pagnez D, Nouaille S, Khrais A, Sayegh FN, Mégarbané A, Loiselet J, Lathrop M, Petit C, Weil D (2002) A novel locus for Usher syndrome type I, USH1G, maps to chromosome 17q24-25. *Hum Genet* 110:348-50.
- Neher (1998) Vesicle pools and Ca²⁺ microdomain: New tools for understanding their roles in neurotransmitter release. *Neuron* 20:389-399.
- Ness SL, Ben-Yosef T, Bar-Lev A, Madeo AC, Brewer CC, Avraham KB, Kornreich R, Desnick RJ, Willner JP, Friedman TB, Griffith AJ (2003) Genetic homogeneity and phenotypic variability among Ashkenazi Jews with Usher syndrome type III. *J Med Genet* 40:767-772.
- Nouvian R, Beutner D, Parsons TD, Moser T (2006) Structure and function of the hair cell ribbon synapse. *J Membr Biol*. 209:153-165.
- Nouvian R, Neef J, Bulankina AV, Reisinger E, Pangršič T, Frank T, Sikorra S, Brose N, Binz T, Moser T (2011) Exocytosis at the hair cell ribbon synapse apparently operates without neuronal SNARE proteins. *Nat Neurosci* 14:411-143.
- Oliver D, Klöcker N, Schuck J, Baukowitz T, Ruppertsberg JP, Fakler B (2000) Gating of Ca²⁺-activated K⁺ channels controls fast inhibitory synaptic transmission at auditory outer hair cells. *Neuron* 26:595-601.
- Oliver D, Knipper M, Derst C, Fakler B (2003) Resting potential and submembrane calcium concentration of inner hair cells in the isolated mouse cochlea are set by KCNQ-type potassium channels. *J Neurosci* 23:2141-2149.
- Oliver D, Taberner AM, Thurm H, Sausbier M, Arntz C, Ruth P, Fakler B, Liberman MC (2006) The role of BK_{Ca} channels in electrical signal encoding in the mammalian auditory periphery. *J Neurosci* 26:6181-6189.
- Pangršič T, Lasarow L, Reuter K, Takago H, Schwander M, Riedel D, Frank T, Tarantino LM, Bailey JS, Strenzke N, Brose N, Müller U, Reisinger E, Moser T (2010) Hearing requires otoferlin-dependent efficient replenishment of synaptic vesicles in hair cells. *Nat Neurosci* 13:869-876.

References

- Pelkey KA, McBain CJ (2008) Target-cell-dependent plasticity within the mossy fibre-CA3 circuit reveals compartmentalized regulation of presynaptic function at divergent release sites. *J Physiol* 586:1495-1502.
- Pieke-Dahl S, Möller CG, Kelley PM, Astuto LM, Cremers CW, Gorin MB, Kimberling WJ (2000) Genetic heterogeneity of Usher syndrome type II: localisation to chromosome 5q. *J Med Genet* 37:256-262.
- Pietola L, Aarnisalo AA, Abdel-Rahman A, Västinsalo H, Isosomppi J, Löppönen H, Kentala E, Johansson R, Valtonen H, Vasama JP, Sankila EM, Jero J (2012) Speech recognition and communication outcomes with cochlear implantation in Usher syndrome type 3. *Otol Neurotol* 33:38-41.
- Platzer J, Engel J, Schrott-Fischer A, Stephan K, Bova S, Chen H, Zheng H, Striessnig J (2000) Congenital deafness and sinoatrial node dysfunction in mice lacking class D L-type Ca²⁺ channels. *Cell* 102:89-97.
- Purves D, Augustine GJ, Fitzpatrick D, Hall WC, LaMantia AS, McNamara JO, Williams SM (2004) *Neuroscience Third Edition*. Sinauer Associates, Inc.
- Ramanathan K, Michael TH, Jiang GJ, Hiel H, Fuchs PA (1999) A molecular mechanism for electrical tuning of cochlear hair cells. *Science* 283:215-217.
- Raphael Y, Altschuler RA (2003) Structure and innervation of the cochlea. *Brain Res Bull* 60:397-422.
- Roberts WM, Jacobs RA, Hudspeth AJ (1990) Colocalization of ion channels involved in frequency selectivity and synaptic transmission at presynaptic active zones of hair cells. *J Neurosci* 10:3664-3684.
- Roux I, Safieddine S, Nouvian R, Grati M, Simmler MC, Bahloul A, Perfettini I, Le Gall M, Rostaing P, Hamard G, Triller A, Avan P, Moser T, Petit C (2006) Otoferlin, defective in a human deafness form, is essential for exocytosis at the auditory ribbon synapse. *Cell* 127:277-289.
- Ruel J, Nouvian R, Gervais d'Aldin C, Pujol R, Eybalin M, Puel JL (2001) Dopamine inhibition of auditory nerve activity in the adult mammalian cochlea. *Eur J Neurosci* 14:977-986.

References

- Rutherford MA, Pangršič T (2012) Molecular anatomy and physiology of exocytosis in sensory hair cells. *Cell Calcium* (in press).
- Sadeghi M, Cohn ES, Kimberling WJ, Tranebjaerg L, Moller C (2005) Audiological and vestibular features in affected subjects with USH3: a genotype/phenotype correlation. *Int J Audiol* 44: 307–316.
- Sankila EM, Pakarinen L, Kääriäinen H, Aittomäki K, Karjalainen S, Sistonen P, de la Chapelle A (1995) Assignment of an Usher syndrome type III (USH3) gene to chromosome 3q. *Hum Mol Genet* 4:93-98.
- Schmitz F, Königstorfer A, Südhof TC (2000) RIBEYE, a component of synaptic ribbons: a protein's journey through evolution provides insight into synaptic ribbon function. *Neuron* 28, 857–872.
- Schnee ME, Ricci AJ (2003) Biophysical and pharmacological characterization of voltage-gated calcium currents in turtle auditory hair cells. *J Physiol* 549:697-717
- Schoch S, Castillo PE, Jo T, Mukherjee K, Geppert M, Wang Y, Schmitz F, Malenka RC, Südhof TC (2002) RIM1 α forms a protein scaffold for regulating neurotransmitter release at the active zone. *Nature* 415:321-326.
- Schoch S, Gundelfinger ED (2006) Molecular organization of the presynaptic active zone. *Cell Tissue Res* 326:379-391.
- Schoch S MT, Kaeser PS, Padgett D, Feldmann N, Chevaleyre V, Castillo PE, Hammer RE, Han W, Schmitz F, Lin W, Südhof TC (2006) Redundant functions of RIM1a and RIM2 α in Ca²⁺-triggered neurotransmitter release. *EMBO J* 25:5852-5863.
- Schwarz K, Natarajan S, Kassas N, Vitale N, Schmitz F (2011) The synaptic ribbon is a site of phosphatidic acid generation in ribbon synapses. *J Neurosci* 31:15996-16011.
- Sendin G, Bulankina AV, Riedel D, Moser T (2007) Maturation of ribbon synapses in hair cells is driven by thyroid hormone. *J Neurosci* 27:3163-3173.
- Shaw EAG (1974) The external ear. In: Keidel W D, and Neff WD (Eds.) *Auditory System: Anatomy Physiology (Ear)*. Berlin: Springer-Verlag.
- Siemens J, Lillo C, Dumont RA, Reynolds A, Williams DS, Gillespie PG, Müller U (2004) Cadherin 23 is a component of the tip link in hair-cell stereocilia. *Nature* 428:950-955.

References

- Simmons DD (2002) Development of the inner ear efferent system across vertebrate species. *J Neurobiol* 53:228-250.
- Simsek-Duran F, Linden DJ, Lonart G (2004) Adapter protein 14-3-3 is required for a presynaptic form of LTP in the cerebellum. *Nat Neurosci* 7:1296-1298.
- Sobin A, Flock A (1983) Immunohistochemical identification and localization of actin and fimbrin in vestibular hair cells in the normal guinea pig and in a strain of the waltzing guinea pig. *Acta Otolaryngol* 96:207-214.
- Söllner C, Rauch GJ, Siemens J, Geisler R, Schuster SC, Müller U, Nicolson T (2004) Mutations in cadherin 23 affect tip links in zebrafish sensory hair cells. *Nature* 428:955-959.
- Smith RJ, Berlin CI, Hejtmancik JF, Keats BJ, Kimberling WJ, Lewis RA, Moller CG, Pelias MZ, Tranebjaerg L (1994) Clinical diagnosis of the Usher syndromes. Usher Syndrome Consortium. *Am J Med Genet* 50:32-38.
- Spoendlin H (1972) Innervation densities of the cochlea. *Acta Otolaryngol.* 73:235-248.
- Sterling P, Matthews G (2005) Structure and function of ribbon synapses. *Trends Neurosci* 28:20-29.
- Südhof TC, Rizo J (2011) Synaptic vesicle exocytosis. *Cold Spring Harb Perspect Biol* 3. pii: a005637.
- Tian G, Zhou Y, Hajkova D, Miyagi M, Dinculescu A, Hauswirth WW, Palczewski K, Geng R, Alagramam KN, Isosomppi J, Sankila EM, Flannery JG, Imanishi Y (2009) Clarin-1, encoded by the Usher Syndrome III causative gene, forms a membranous microdomain: possible role of clarin-1 in organizing the actin cytoskeleton. *J Biol Chem* 284:18980-18993.
- tom Dieck S, Altrock WD, Kessels MM, Qualmann B, Regus H, Brauner D, Fejtová A, Bracko O, Gundelfinger ED, Brandstätter JH (2005) Molecular dissection of the photoreceptor ribbon synapse: physical interaction of Bassoon and RIBEYE is essential for the assembly of the ribbon complex. *J Cell Biol* 168:825-836.
- Tritsch NS, Yi E, Gale JE, Glowatzki E, Bergles DE (2007) The origin of spontaneous activity in the developing auditory system. *Nature* 450:50-55.

References

- Usher C (1914) On the inheritance of retinitis pigmentosa with notes of cases. *R Lond Ophthalmol Hosp Rep* 19:130–236.
- Verpy E, Leibovici M, Zwaenepoel I, Liu XZ, Gal A, Salem N, Mansour A, Blanchard S, Kobayashi I, Keats BJ, Slim R, Petit C (2000) A defect in harmonin, a PDZ domain-containing protein expressed in the inner ear sensory hair cells, underlies Usher syndrome type 1C. *Nat Genet* 26:51-55.
- Vetter DE, Katz E, Maison SF, Taranda J, Turcan S, Ballestero J, Liberman MC, Elgoyhen AB, Boulter J (2007) The alpha10 nicotinic acetylcholine receptor subunit is required for normal synaptic function and integrity of the olivocochlear system. *Proc Natl Acad Sci U S A* 104:20594-20599.
- Vetter DE, Liberman MC, Mann J, Barhanin J, Boulter J, Brown MC, Saffiote-Kolman J, Heinemann SF, Elgoyhen AB (1999) Role of alpha9 nicotinic ACh receptor subunits in the development and function of cochlear efferent innervation. *Neuron* 23:93–103.
- von Békésy G. DC resting potentials inside the cochlear partition. *J Acoust Soc Am.* 1952;24:72–76.
- von Graefe A (1858) Vereinzelt Beobachtungen und Bemerkungen Exceptionelle Verhalten des Gesichtsfeldes bei Pigmentenartung des Netzhaut. *Arch Klin Ophthalmol* 4:250–253.
- Wang Y, Okamoto M, Schmitz F, Hofmann K, Südhof TC (1997) Rim is a putative Rab3 effector in regulating synaptic-vesicle fusion. *Nature* 388:593-598.
- Wang Y, Sugita S, Südhof TC (2000) The RIM/NIM family of neuronal C2 domain proteins. Interactions with Rab3 and a new class of Src homology 3 domain proteins. *J Biol Chem.* 275, 20033-20044.
- Wangemann P, Schacht J. Homeostatic mechanisms in the cochlea. In Springer Handbook of Auditory Research, Vol.8: The Cochlea, ed. Dallos P, Popper AN, Fay R, p130-185. Springer-Verlag, New York.
- Wayne S, Der Kaloustian VM, Schloss M, Polomeno R, Scott DA, Hejtmancik JF, Sheffield VC, Smith RJ (1996) Localization of the Usher syndrome type ID gene (Ush1D) to chromosome 10. *Hum Mol Genet* 5:1689-1692.

References

- Weil D, Blanchard S, Kaplan J, Guilford P, Gibson F, Walsh J, Mburu P, Varela A, Levilliers J, Weston MD, Kelley PM, Kimberling WJ, Wagenaar M, Levi-Acobas F, Larget-Piet D, Munnich A, Steel KP, Brown SDM, Petit C (1995) Defective myosin VIIIA gene responsible for Usher syndrome type 1B. *Nat Genet* 374:60–61.
- Weil D, El-Amraoui A, Masmoudi S, Mustapha M, Kikkawa Y, Lainé S, Delmaghani S, Adato A, Nadifi S, Zina ZB, Hamel C, Gal A, Ayadi H, Yonekawa H, Petit C (2003) Usher syndrome type I G (USH1G) is caused by mutations in the gene encoding SANS, a protein that associates with the USH1C protein, harmonin. *Hum Mol Genet* 12:463-471.
- Weisz C, Glowatzki E, Fuchs P (2009) The postsynaptic function of type II cochlear afferents. *Nature* 461:1126-1129.
- Weston MD, Luijendijk MW, Humphrey KD, Möller C, Kimberling WJ (2004) Mutations in the VLGR1 gene implicate G-protein signaling in the pathogenesis of Usher syndrome type II. *Am J Hum Genet* 74:357-366.
- Wever EG, Lawrence M (1954) *Physiological Acoustics*. Princeton, Princeton U.P.
- White PM, Doetzlhofer A, Lee YS, Groves AK, Segil N (2006) Mammalian cochlear supporting cells can divide and trans-differentiate into hair cells. *Nature* 441:984-987.
- Yang PS, Alseikhan BA, Hiel H, Grant L, Mori MX, Yang W, Fuchs PA, Yue DT (2006) Switching of Ca²⁺-dependent inactivation of Ca(v)1.3 channels by calcium binding proteins of auditory hair cells. *J Neurosci* 26:10677-10689.
- Yuhas WA, Fuchs PA (1999) Apamin-sensitive, small-conductance, calcium-activated potassium channels mediate cholinergic inhibition of chick auditory hair cells. *J Comp Physiol A* 185:455-462.
- Zallocchi M, Meehan DT, Delimont D, Askew C, Garige S, Gratton MA, Rothermund-Franklin CA, Cosgrove D (2009). Localization and expression of clarin-1, the *Clrn1* gene product, in auditory hair cells and photoreceptors. *Hear Res* 255:109-120.
- Zallocchi M, Meehan DT, Delimont D, Rutledge J, Gratton MA, Flannery J, Cosgrove D (2012) Role for a novel Usher protein complex in hair cell synaptic maturation. *PLoS One* 7:e30573.

References

- Zampini V, Johnson SL, Franz C, Lawrence ND, Münkner S, Engel J, Knipper M, Magistretti J, Masetto S, Marcotti W (2009) Elementary properties of CaV1.3 Ca(2+) channels expressed in mouse cochlear inner hair cells. *J Physiol* 588:187-199.
- Zenisek D, Davila V, Wan L, Almers W (2003) Imaging calcium entry sites and ribbon structures in two presynaptic cells. *J Neurosci* 23:2538-2548.
- Zheng J, Shen W, He DZ, Long KB, Madison LD, Dallos P (2000) Prestin is the motor protein of cochlear outer hair cells. *Nature* 405:149-155.

References

Abbreviations

ABR	Auditory brainstem response
ACh	Acetylcholine
BK channel	Large conductance voltage and Ca ²⁺ activated K ⁺ channel
C _m	Membrane capacitance
ΔC _m	Membrane capacitance increment
CN	Cochlear nucleus
CtBP	C-terminal binding protein
DPOAE	Distortion-product otoacoustic emission
EGTA	Ethylene glycol-bis-(2-aminoethyl)-N,N,N',N'-tetraacetic acid
GluR	Glutamate receptor
GSDB	Goat serum diluted buffer
GTP	Guanosine 5'-triphosphate
HEPES-HBSS	HEPES-buffered Hanks' balanced salts solution
IBa	Ba ²⁺ current
ICa	Ca ²⁺ current
IV	Current-voltage relationship
IHC	Inner hair cell
LOC	Lateral olivocochlear
MET	Mechanoelectrical transduction
MOC	Medial olivocochlear
MSO	Medial superior olive
OHC	Outer hair cell
PBS	Phosphate-buffered saline
PSTH	Poststimulus time histogram
RIM	Rab3 interacting molecule
RRP	Readily releasable pool
RS	Series resistance
RT-PCR	Reverse transcription polymerase chain reaction

Abbreviations

SGN	Spiral ganglion neuron
SK2	Small conductance Ca ²⁺ activated K ⁺ channel
SNARE	Soluble NSF attachment protein receptor
SOC	Superior olivary complex
SPL	Sound pressure level
TEA-Cl	Tetraethylammonium chloride
VGCC	Voltage-gated Ca ²⁺ channel
WT	Wild-type

Acknowledgements

6. Acknowledgements

I would like to thank Prof. Dr. Tobias Moser for providing me an opportunity to engage in this project as well as for his excellent instruction and continuous support.

I also would like to thank Dr. Nicola Strenzke for enthusiastically mentoring me to stand up against many challenges and difficulties.

I feel very grateful to the members of the PhD thesis committee, Prof. Dr. Martin Göpfert and Prof. Dr. Georg Klump, for their valuable advices

I also feel very grateful to Prof. Dr. Stefan Treue (University of Oldenburg) for providing me an honor to become one of the first PhD students to receive a fellowship of the NEUROSENSES program. I also thank to Ms. Karin Peinemann for supporting me from the administrative work in this fellowship.

Further, I would like to express gratitude to the GGNB administrative office, especially to Ms. Kirsten Pöhlker for her helps to all kinds of administrative issues relevant to me.

I appreciate collaborators in the RIM project; first of all Dr. Friederike Predöhl (InnerEarLab) for her excellent partnership, excellent molecular biological technique, and insights into especially molecular biological part of this study. Without her contribution, this work was not able to be achieved. I would like to pay my best respect and send my appreciation to her. Dr. Jakob Neef (InnerEarLab) for everything. His continuous supports and helps from the very beginning when I started to work on inner hair cells, were always helpful. Dr. Anna Bulankina for the preliminary work of molecular biological investigation of active zone proteins in the inner hair cells and her comments. Dr. Sonja Wojcik, (MPIEM) for courtesy of cre mice line and suggestions over the breeding strategy. Prof. Dr. Susanne Schoch (University of Bonn) for courtesy of RIM 2 α knockout mice, lab-made antibodies and her implicative suggestions over this project, Prof. Dr. Pascal Kaeser (Harvard Medical School, USA) and Prof. Dr. Thomas Südhof (Stanford University, USA) for courtesy of RIM 1/2 double floxed mice and their helpful suggestions. I also appreciate collaborators in the clarin-1 project; Prof. Dr. Kumar Alagramam, Dr. Ruishuang Geng, Dr. Sami Melki, Dr. Daniel H.-C. Chen, Dr. Guilian Tian, Prof. Dr. Yoshikazu Imanishi (Case Western Reserve

Acknowledgements

University), Dr. David Furness (Keele University, UK), Dr. Charles Askew, Dr. Geoff Horwitz (University of Virginia, USA), and Prof. Dr. Jeffrey Holt (Harvard Medical School, USA).

In addition, I would like to express many thanks to my colleagues in the InnerEarLab for their helps and discussions, especially to Dr. Anna Gehrt for showing how to address the auditory nerves in the single-unit recording, Mr. Alejandro M. Schulz for his cooperation in our joint method courses, as well as Ms. Nadine Hermann and Mr. Stefan Thom for helping the ABR recordings. Also I would like to show my special thanks to Ms. Christiane Senger-Freitag and Ms. Sandra Gerke for their wonderful assistance to this work. I also express my gratitude to animal care takers in animal facilities.

My present work is greatly indebted to critical advices from Prof. Dr. Tomoyuki Takahashi, Dr. Tetsuya Hori, Dr. Yukihiro Nakamura (Doshisha University and Okinawa institute of Science and Technology, Japan), Prof. Dr. Taro Ishikawa (Jikei University, Japan), Prof. Dr. Masao Tachibana (University of Tokyo, Japan), Prof. Dr. Takeshi Sakaba (Doshisha University, Japan), Prof. Dr. Nobutake Hosoi (Gunma University, Japan) , Prof. Dr. Toshihisa Ohtsuka (Yamanashi University, Japan) and Dr. Jeong Seop Rhee (MPIEM). Their insightful comments and indications were very helpful and shed a light on this work. I sincerely express my respect and gratitude to them.

Finally, I am thankful to my father Minoru Oshima, My mother Nakako Oshima, and my husband Dr. Hideki Takago, without whose warm-hearted supports and deep and unlimited faith, I have never fulfilled this work. I would like to dedicate my best gratitude, respect and love.

Curriculum Vitae

7. Curriculum Vitae

[Name]

Tomoko Oshima-Takago, B.A. in Biology, M.Sc. in Medical Sciences.

[Current Address]

InnenOhrLabor, HNO-Klinik, Universitätsmedizin Göttingen

Robert-Koch Str. 40, D-37075, Göttingen, Germany

Tel: +41-551-39-22837

Fax: +41-551-39-12950

E-mail: toshima@gwdg.de

[Personal information]

Date of Birth: 12 August, 1981

Nationality: Japan

Curriculum Vitae

[Academic education & Professional career]

Undergraduate education

2000 - 2004 International Christian University (ICU), College of Liberal Arts.
2004 B.A. in Biology (ICU)

Graduate education

2005 - 2007 Master course program of Medical Sciences, Graduate school of
Medicine, University of Tokyo, Japan.
2007 M.Sc. in Medical Sciences (University of Tokyo)
2007 - 2009 Enrolled in the Ph.D. course of functional biology,
Graduate School of Medicine, University of Tokyo.
2009 March - Present
Member of the Inner Ear Lab, Göttingen Graduate School for
Neurosciences and Molecular Biosciences (GGNB), Georg August
University of Göttingen.

Professional Career

2004 October – 2005 March
Assistant technician at Gene Research Center,
Tokyo University of Agriculture and Technology.

[Master thesis]

“Auditory activity dependence in the developmental changes of glycinergic inhibitory synaptic currents”

This thesis was carried out under the supervision of Prof. Dr. Tomoyuki Takahashi, Department of Neurophysiology, Graduate School of Medicine, University of Tokyo.

[Scholarship]

“NEUROSENSES, PhD training in Integrative Neurosensory Sciences” sponsored by Niedersächsisches Ministerium Für Wissenschaft und Kultur, Hannover

Curriculum Vitae

[Publication]

Geng R, Melki S, Chen D, Tian G, Furness D, Oshima-Takago T, Neef J, Moser T, Askew C, Horwitz G, Holt J, Imanishi Y, Alagramam KN (2012) The Mechanosensory Structure of the Hair Cell Requires Clarin-1, a Protein Encoded by Usher Syndrome III Causative Gene. J Neurosci 32:9485-9498.

[Presentation]

Oshima-Takago T, Predöhl F, Schoch S, Südhof T, Neef J, Strenzke N, Moser T. Probing expressions and functions of RIM proteins in the inner hair cell. OIST Symposium "Molecular & Structural Organization of Presynaptic Function and Plasticity" 7-9 September.2011, Okinawa Institute of Science and Technology, Uruma, Japan.

Oshima-Takago T, Predöhl F, Schoch S, Südhof T, Neef J, Strenzke N, Moser T. Probing expressions and functions of RIM proteins in the inner hair cell. 19-21 September 2011, Max-Planck-Institute for Experimental Medicine, Göttingen, Germany.

Oshima-Takago T, Predöhl F, Schoch S, Südhof T, Neef J, Strenzke N, Moser T. Probing expressions and functions of RIM in the inner hair cell. The 89th Annual Meeting of Physiological Society of Japan. 29 March 2012, Matsumoto, Japan.

Oshima-Takago T, Predöhl F, Schoch S, Südhof T, Neef J, Strenzke N, Moser T. Probing expressions and functions of RIM in the inner hair cell. The 35th Annual Meeting of the Japan Neuroscience Society. 19 September 2012, Nagoya, Japan.

[Lecture]

Oshima-Takago T, Schulz AM, Moser T. GGNB short methods courses: Basics of electrophysiological measurements in slice preparations. 8-9 March 2012, InnerEarLab, Department of Otolaryngology, UMG Göttingen.

Oshima-Takago T, Rhee JS. Nerve cell culture and patch-clamp recordings from nerve cells. 19-20 March 2012, Max-Planck Institute for Experimental Medicine.

Curriculum Vitae

Oshima-Takago T, Rhee JS. Nerve cell culture and patch-clamp recordings from nerve cells. 24-25 September 2012, Max-Planck Institute for Experimental Medicine.

Oshima-Takago T, Picher MM, Moser T. GGNB short methods courses: Basics of electrophysiological measurements in slice preparations and cell cultures. 11-12 October 2012, InnerEarLab, Department of Otolaryngology, UMG Göttingen.